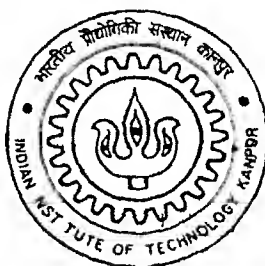


MODELING AND SIMULATION OF ORGANIC LIGHT EMITTING DIODE (OLED)

By

Flt Lt C G NARASIMHA PRASAD

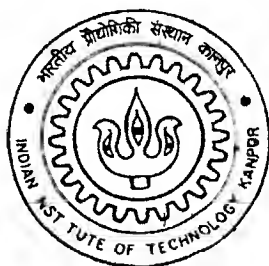


DEPARTMENT OF ELECTRICAL ENGINEERING
Indian Institute of Technology Kanpur
JANUARY 2002

MODELING AND SIMULATION OF ORGANIC LIGHT EMITTING DIODE (OLED)

By

Flt Lt C G NARASIMHA PRASAD



DEPARTMENT OF ELECTRICAL ENGINEERING
Indian Institute of Technology Kanpur
JANUARY 2002

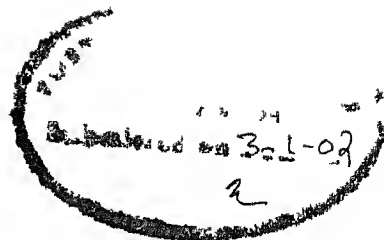
- 4 MAR 2002 / EE

पुरुषोत्तम काशीनाथ कैलकर पुस्तकालय
भारतीय प्रौद्योगिकी संस्थान कानपुर
अवाप्ति क्र० A...137891.....



A137891

CERTIFICATE



This is to certify that the work contained in the thesis titled **Modeling and Simulation of Organic Light Emitting Diode (OLED)** ' by Flt Lt C G Narasimha Prasad (Roll No Y010408) has been done under my supervision and that this work has not been submitted elsewhere for a degree

Jan2002

Dr Baquer Mazhar

Associate Professor

Department of Electrical Engineering

Indian Institute of Technology

Kanpur 208016

India

ACKNOWLEDGEMENTS

This thesis grew out of a series of dialogues with my thesis supervisor Dr B Mazhari. His probing questions enabled me to grasp the complexity of the subject. His great efforts to explain things clearly and simply are always remembered. I am thankful to his excellent guidance.

I am indebted to Dr R Sharan whose course work inspired me to explore the area of Organic Light Emitting Diode. His words of encouragement helped me to achieve my goal.

I am thankful to my parent organization Indian Air Force for providing me financial support.

Many thanks to my student colleagues of VLSI lab for providing me a stimulating environment to work.

I wish to thank my parents and sister for inspiring me to undertake this course.

Lastly my deepest gratitude to my son Avi and wife Karpagam without whose love and support I could not have completed this work. It is wonderful to do this work with both of you!

So I close by thanking god for getting me through this phase of life.

Flt Lt C G N Prasad

ABSTRACT

This work describes the simulation and modeling of current voltage characteristics of polymer light emitting diode. To understand the device characteristics first a single layer organic device with single carrier injection is studied. The simulations are used to clarify the role of barrier height, device thickness and mobility. A new analytical model is developed based on a simple mobility model that matches well with the experimental characteristic. It is shown that in a single layer OLED with both electron and hole injection recombination takes place primarily near the cathode due to the much smaller electron mobility. It is also shown that with the proper adjustment of the anode barrier height recombination is spread uniformly over the bulk. In the two layer device, presence of barrier at the organic-organic interface results in most of the recombination taking place at the interface of two organic layers. It is shown that to get good device efficiency hole barrier at the interface should be sufficiently large and greater than 0.3 eV. Electron barrier at the interface however plays no significant role. It is also shown that the electron transport layer largely determines turn on voltage of the device.

**DEDICATED TO MY
AJJI**

CONTENTS

1 Introduction

1 1 Evolution of OLED Display	1
1 2 OLED Display	3
1 2 1 Passive Matrix	4
1 2 2 Active Matrix	5
1 3 Scope of the Thesis	5
1 4 Organization of The Thesis	6

2 Literature Review

2 1 Introduction	7
2 2 OLED Structure	7
2 3 Device Characteristics	8
2 4 Tunneling	10
2 5 Space Charge Limited Current (SCLC)	10
2 6 Space Charge Limited Current With Traps	11
2 7 Field Dependent Mobility	12

3 Simulation of Single Carrier Device

3 1 Single Carrier Device	13
3 2 Effect of Schottky barrier on current flow	14
3 3 Bulk limited current voltage characteristic	15
3 4 Device modeling in high current region using theory of SCLC	18
3 5 Experimental and simulation results	21
3 6 Model for SCLC with field dependent mobility of the form	
$\mu = \mu_0 \left(\frac{E}{E_0} \right)$	22
3 7 Device modeling in low current region	25
3 8 Contact limited current flow ($\phi_{BH} > 0.15$ eV)	29
3 9 Criteria for distinguishing bulk limited and contact limited current	33

3 10 Single Layer Bipolar Device	35
3 11 Recombination	36
3 12 Effect Of hole injection Barrier on recombination profile	40
4 Double Layer Device	
4 1 Energy Band Picture	41
4 2 Effect of thickness of CN_PPV layer on J V characteristic	42
4 3 Organic organic interface barrier	46
4 4 Comparison of device efficiencies	49
5 Conclusions and Future Scope of the Thesis	
5 1 Conclusion	50
5 2 Application of the work	50
5 3 Future scope of the thesis	51
References	52
Appendix-A	53

LIST OF SYMBOLS

E	Electric Field
J	Current Density
J_p	Hole Current Density
J_n	Electron Current Density
n	Electron Carrier Concentration
p	Hole Carrier Concentration
q	Magnitude of Electron Charge
U	Total Rate of Recombination
ε	Permittivity ($=\varepsilon_r \varepsilon_0$)
μ_p	Hole Mobility
μ_n	Electron Mobility
χ	Electron Affinity
ϕ_h	Barrier Height Seen by Hole while coming from Metal to Organic Material
ϕ_n	Barrier Height Seen by Electron while coming from Metal to Organic Material

LIST OF FIGURES

Fig 1 1 An Organic Passive Matrix Display	3
Fig 1 2 Display matrix Block Diagram	4
Fig 2 1 Structure of OLED	8
Fig 2 2 Mechanism of Light Emission in OLED	9
Fig 2 3 Energy Band Diagram of the Metal Insulator	11
Fig 3 1 Single Carrier OLED Structure	13
Fig 3 2 J V Characteristics of Single carrier Device	14
Fig 3 3 Curve Fitting to calculated J V characteristic	16
Fig 3 4 Hole Density Profile of the device in Space Charge Limited Regime	17
Fig 3 5 Electric Field Profile of the device in Space Charge Limited Regime	17
Fig 3 6 Comparison of J V characteristics	20
Fig 3 7 Calculated and Experimental J V of Pt/MEH PPV/Al Device	21
Fig 3 8 Curve fitting to estimate the Value of n	23
Fig 3 9 Comparison of J V characteristics of Murgatroyd Model and New model	25
Fig 3 10 Low Current Region J V	26
Fig 3 11 Cross section of the Device	26
Fig 3 12 Electric Field Profile at an applied bias of 0.2V	27
Fig 3 13 J V Characteristic of Contact limited device	30
Fig 3 14 Experimental and Calculated J V characteristic of a contact limited device	30
Fig 3 15 Calculated Electric Field Profile of a contact limited device	32
Fig 3 16 Calculated Hole Profile of a contact limited device	32
Fig 3 17 Thickness Dependence of current Density	33
Fig 3 18 Dependence of Current on voltage of a contact limited device	34
Fig 3 19 Energy Band Diagram of a Single Layer Device	35
Fig 3 20 Calculated and Experimental J V of Single Layer Bipolar Device	37
Fig 3 21 Recombination Profile of a Single Layer Bipolar Device	38
Fig 3 22 Carrier Density Profile of a Single Layer Bipolar Device	38
Fig 3 23 Recombination rate and Carrier Profile of a Bipolar Device with a mobility ratio 10	39
Fig 3 24 Recombination Profile of a Bipolar Device with varying hole injecting barrier	40
Fig 4 1 Energy Band Diagram of a double Layer device	41
Fig 4 2 Recombination Profile of a double layer Device	43
Fig 4 3 Carrier Profile of Double layer hole only device	43

Fig 4 4 Potential variation in a double Layer device	44
Fig 4 5 J V Plot of Different Devices	45
Fig 4 6 Energy band diagram of a b1 layer device	46
Fig 4 7 Carrier profile of a double layer at an applied bias of 5V	47
Fig 4 8 Plot of the device efficiency as a function of hole barrier at the interface	48

LIST OF TABLES

Table 4 1 Double layer devices of varying layer thickness	44
Table 4 2 Device efficiencies at different hole barrier heights	47
Table 4 3 Device efficiencies at different electron barrier heights	48
Table 4 4 Comparison of device efficiency	49

Chapter 1

Introduction

1.1 Evolution of the OLED display

The rise in importance of the electronic displays over the last forty years has been a direct consequence of the explosive proliferation of computers of all sizes from the large mainframes of the 1960s and 1970s to the small handheld systems of the late 1990s. Initially displays based on neon discharges were used to display binary and decimal digits but these quickly gave way to displays which exploited cathode ray tubes (CRT) developed for television. Because of the economies of scale afforded by the huge television market the CRT still represents nearly half of the information display market in terms of units. In spite of the fact that the CRT is still the most economical technology for display it has never been able to shed its most serious drawback of weight and volume.

For this reason even in the early days of television engineers dreamed of making thin light flat panel displays that would capture the function of the CRT in a more attractive package perhaps even one that would be easily portable. Therefore numerous flat panel display technologies such as liquid crystal display (LCD) light emitting diode (LED) organic light emitting diode (OLED) plasma display panel (PDP) have been developed. Unfortunately the first major commercial flat panel technology based again on neon discharge (plasma display) was not when introduced was economically competitive with the CRTs it was intended to replace. As desktop displays they were too expensive and lacked the ability to render full color. For portable applications they were too heavy and too inefficient. Plasma displays are now the serious competitors in the race for the market of large size hanging high definition television monitors (HDTV).

Advent of personal computers in the early 1980s prompted everyone to look for a way to make a portable version. Display attention shifted to liquid crystal displays (LCDs) which already had gained reputation in watches for low power demands and low weight. Early screen images produced on liquid crystal flat panels were grossly inferior to CRT images even though the computers incorporating them were highly portable. In 1983 LCD display with image characteristics of a color CRT was brought in. Within five years this technology had been

developed to a point at which display suitable for portable computers became feasible. They are not competitive in cost with CRT technology.

Therefore there was a need of a flat panel display which is cost effective and with features of a conventional CRT display. Thus started display based on organic light emitting diode commonly called OLED. An OLED is an electronic device made by placing a series of organic thin films between two conductors. When electrical current is applied, a bright light is emitted. OLEDs are lightweight, durable, power efficient and ideal for portable applications. OLEDs have fewer process steps and also use both fewer and lower cost materials than LCD displays. Active matrix OLED displays are expected to replace LCDs in most flat panel display applications. Unlike power hungry LCD displays, OLED displays are brighter, sharper, power friendly and offer viewing angles of up to 170 degrees. If you've ever sat on an airplane with a conventional LCD display, you know that it is very difficult to see the movie if you're off center at all from that display. OLED displays don't have that restriction. OLEDs can replace the current technology in many applications due to the following performance advantages over LCDs:

- Greater brightness
- Faster response time for full motion video
- Fuller viewing angles
- Lighter weight
- Greater environmental durability
- More power efficiency
- Broader operating temperature ranges
- Greater cost effectiveness

The first commercial GaAsP light emitting diodes (LEDs) were introduced in 1962. Electroluminescence (EL) was reported in organic materials at about the same time from experiments. Development of the display products was hampered by fabrication, packaging and reliability problems. So progress over the next two decades were in inorganic area. Mainly Tang

and Van Slyke in 1987 [4] revived the interest in organic EL with their first multi layer device. An explosive growth of activity followed in both academia and industry.

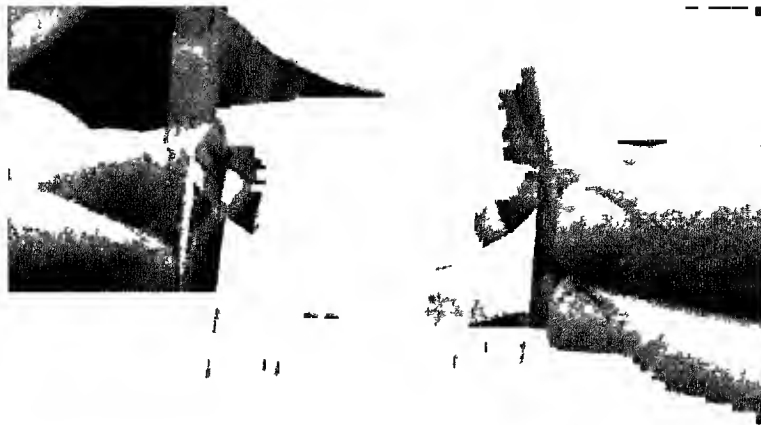


Figure 1.1 An organic passive matrix display on a substrate of polyethylene terephthalate, a lightweight plastic, will bend around a diameter of less than a centimeter. The 18 mm thick, 5 by 10 cm monochrome display consists of 128 by 64 pixels, each measuring 400 by 500 μm , and is being operated at conventional video brightness of 100 cd/m^2 . It was fabricated by Universal Display Corp., Ewing, NJ, with a moisture barrier built into the plastic that prevents degradation of the pixels.

1.2 OLED Display

Display is an array of independently controllable pixels. Each individual pixel is an OLED. Number of pixels depends on dimension and resolution required by a particular application. For example, an NTSC standard TV screen requires 10^5 pixels. Addressing large number of pixels in an array is an important issue in display technology. In a matrix addressed display, pixels are organized in rows and columns as shown in **Fig 1.2**. Each pixel is electrically connected between a row lead and column lead.

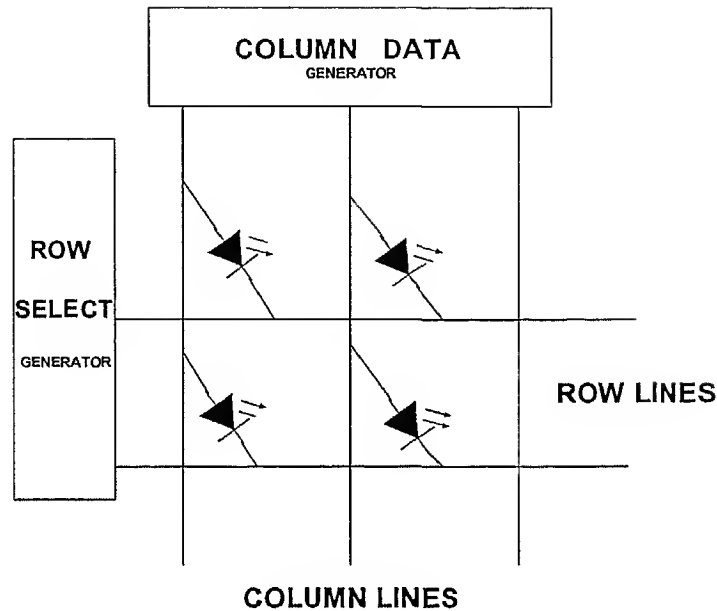


Figure 1 2 Display Matrix

An OLED is a current driven device that is the intensity of the output light is directly proportional to the electrical current flowing through the device. An OLED display therefore requires the control and modulation of electrical current levels through individual elements (pixels) in order to display text or graphic images.

There are two types of OLED display architectures

- (a) Passive matrix
- (b) Active matrix

1 2 1 Passive Matrix

Passive Matrix displays consist of an array of picture elements or pixels deposited on a patterned substrate in a matrix of rows and columns. In an OLED display, each pixel is an organic light emitting diode formed at the intersection of each column and row line. The first OLED displays were addressed as a passive matrix. This means that to illuminate any particular pixel, electrical signals are applied to the row line and column line (the

intersection of which defines the pixel) The more current pumped through each pixel diode the brighter the pixel looks to our eyes

1 2 2 Active Matrix

In an active matrix display the array is still divided into a series of row and column lines with each pixel formed at the intersection of a row and column line However each pixel now consists of an organic light emitting diode (OLED) in series with a thin film transistor (TFT) The TFT is a switch that can control the amount of current flowing through the OLED In an active matrix OLED display (AMOLED) information is sent to the transistor in each pixel telling it how bright the pixel should shine The TFT then stores this information and continuously controls the current flowing through the OLED In this way the OLED is operating all the time avoiding the need for the very high currents necessary in a passive matrix display

Multicolor automobile stereo displays are now available from Pioneer Corp of Tokyo and Royal Philips Electronics NV Amsterdam is gearing up to produce both OLED backlights to be used in LCDs and organic integrated circuits It is possible that soon portable and lightweight roll up OLED displays will cover our walls replacing the bulky and power hungry cathode ray tube that has been the television standard for 50 years

1 3 Scope of the thesis

Organic light emitting diodes (OLED s) have emerged over the past ten years as viable candidates for application in display technologies PPV derivatives were the first polymer to show electroluminescence While the technologies of OLEDs are advancing rapidly fundamental studies of the device operations are lagging behind Optimizing performance of OLED requires understanding of the basic processes like charge injection charge transport and recombination An approach to study the device is to start from a simple device and understanding gained from the simple device can then be applied to a more complex structure

This work describes simulation and modeling of the current voltage characteristic of a polymer light emitting diode To understand the characteristics first a specific case has been considered in which energy barrier to injection of electrons is much larger than those for holes so that the holes dominate the current flow The simulations are used to clarify the role of barrier height device thickness and mobility in determining J V characteristic of the device A new

analytical model is developed based on a simple mobility model. Device calculations of a bipolar single layer OLED are presented. Bipolar devices are of interest because recombination can be investigated. It is shown that in a single layer OLED with both electron and hole injection recombination takes place primarily near the cathode due to much smaller electron mobility. It is also shown that with the proper adjustment of the anode barrier height recombination is spread uniformly over the bulk.

The limitations of a single layer device can be overcome by employing a two organic layer structure. In the two layer device presence of barrier at the organic-organic interface results in most of the recombination taking place at the interface of two organic layers. It is shown that to get a good device efficiency hole barrier at the interface should be sufficiently large and greater than 0.3 eV. Electron barrier at the interface however plays no significant role. It is also shown that the electron transport layer largely determines turn on voltage of the device. Calculated device efficiency is presented for representative cases of device parameters.

1.4 Organization of the thesis

This thesis is organized into five chapters. In chapter 2 a complete review of the various models involved in simulation of a single layer OLED has been discussed. This chapter forms a necessary background on which the present work is based. Chapter 3 is devoted to simulation and modeling of current-voltage characteristics of a polymer light emitting diode. Simulations are carried out using a 1-D device simulator (**SIM WINDOWS**) for single and double layer devices. In chapter 4 results from simulations of a double layer OLED have been presented with the emphasis on organic-organic interface role in determining device efficiency. Finally important results of present work are summarized in Chapter 5.

Chapter 2

Literature review

2.1 Introduction

The observation of efficient electro luminescence in organic semiconductors a decade ago gave a new momentum to the field of organic opto electronics. OLEDs are currently under intense development in both academia and industry for applications in flat panel displays. The first commercial product, a car stereo display, was introduced in market three years ago. Today almost every major consumer electronic company has an experimental program in OLED.

As a result of both easy processing and mechanical flexibility, polymer light emitting diodes are presently considered as suitable candidates for large area applications. The organic materials used to fabricate OLEDs are undoped and quite insulating. They are undoped and essentially have no free carriers at room temperature. Current flow in the device results from the carriers that are injected from the contacts. Mobility of carriers in organic materials is very low, of order of 10^{-6} cm²/V s. They have energy gaps ranging from 1.5 eV to 3.5 eV. A key difference [16] between organic and common inorganic light emitting diodes is in the carrier transport properties in the device. In the former, current is due to injection; in the latter device, current carriers originate from dopants (donors and acceptors). As a result of these differences, the potential and charge profiles in the devices are quite different for the two cases.

2.2 Organic Light Emitting Diode Structure

The *p-n* diode structure proves to be a key feature for the OLED device. The basic structure consists of two layers of organic thin films: a hole transport layer and an electron transport layer sandwiched between an anode and a cathode [Fig 2.1]. Under a dc bias, electrons are injected from a low work function ($\Phi_w=3$ to 4 eV) cathode and holes are injected from a high work function ($\Phi_w=5$ eV) anode into the organic materials. These two organic layers, each of the order of about 500 Å thick, provide the appropriate media for transporting the charge carriers towards the interface formed between the two layers. Sequence of events which result in light is illustrated in Fig 2.2.

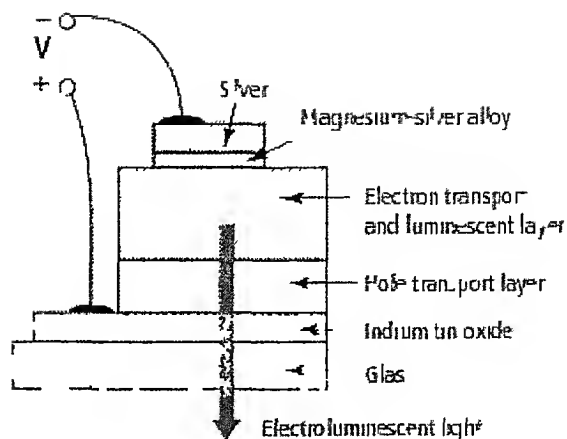


Figure 2.1 Structure of OLED

OLED device can be divided into two classes namely small molecule devices and organic polymer devices. Alq_3 and PPV are two representatives of small molecules and polymers materials respectively. The main difference between the small molecule and polymer materials is in their processing methods and mechanical properties. Small molecule devices are fabricated using vacuum evaporation techniques, whereas polymer structures can be applied using spin coating or even ink jet printing techniques.

2.3 Device characteristics

The operation of the OLED involves four basic steps: charge injection, charge transport, charge recombination, and luminescence. An understanding of the operation of OLED therefore requires knowledge of injection, transport, and recombination processes involved [1]. It is useful to consider an organic diode structure in which one carrier type [2] (either electrons or holes) dominates the current flow in order to understand the charge injection and transport. The understanding gained from simple device can then be applied to more complex devices. Such a single carrier device can be fabricated by choosing contacts such that energy barrier for one kind of carrier is much larger than other. In such devices, recombination does not play a significant role [3]. Experimental study of such single carrier structure has been carried out in [5]. The choice of contacts determines whether the device is electron only or hole only device. PPV derivative is one of the most widely used materials for experiments and simulation (because of larger conversion efficiency).

Sequence of events that result in light when bias is applied is illustrated below

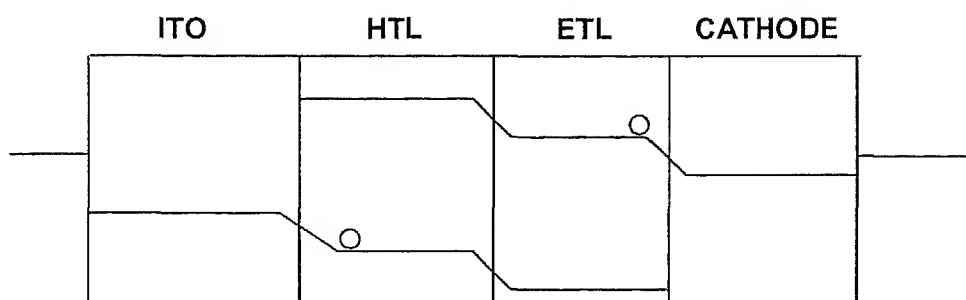


Figure 2 2a An electric field is applied to the device Holes are injected into hole conducting polymer layer At the same time electrons from cathode are injected into electron conducting layer

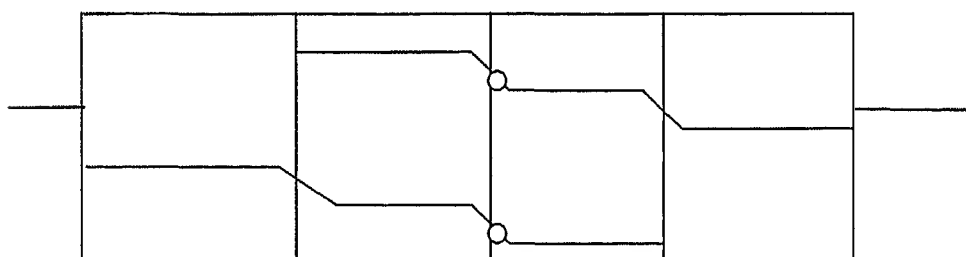


Figure 2 2b Driven by electric field holes and electrons diffuse through the respective layers The mobility of holes being more than that of electrons holes reach HTL/ETL interface earlier

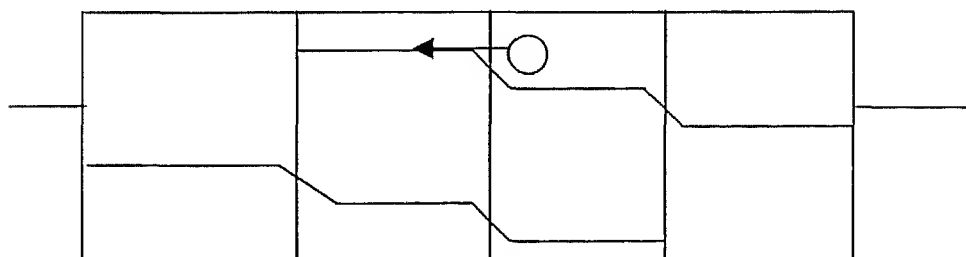


Figure 2 2c when electron and hole come close, they capture one another and form a neutral excited state This form is called exciton Exciton then decays radiatively

In a single carrier device current under extreme conditions can be either contact or bulk limited. In contact limited device injection is determined by following mechanisms

- (a) Thermionic emission with field induced barrier lowering
- (b) Tunneling [5]

In bulk limited device drift and diffusion mechanisms with field dependent mobility and suitable trap distribution are required to explain the device behavior

2.4 Tunneling

Parker [5] has proposed a model in which J-V characteristics of OLED is determined by the Fowler-Nordheim tunneling of both electrons and holes through contact barrier arising from band offset between polymer and electrodes. This model states that holes and electrons are able to tunnel into polymer when sufficiently high applied electric field tilts the polymer band to present sufficiently thin barrier. However quantitatively current predicted by Fowler-Nordheim theory exceeded the experimentally observed currents. Furthermore at low fields the tunneling model was found not to be applicable. In spite of this discrepancy the concept of F-N tunneling became a generally accepted model in order to explain the device performance of OLED. Following this model the device performance of OLED can be improved by balancing the contact barriers of both electrons and holes. An unbalanced injection results in an excess of one carrier type and which does not contribute to light emission. Reduction of the contact barrier leads to more current and a higher light output at equal voltage. Thus in order to obtain efficient device the work function of the cathode and anode should be close to conduction and valence band of the organic material.

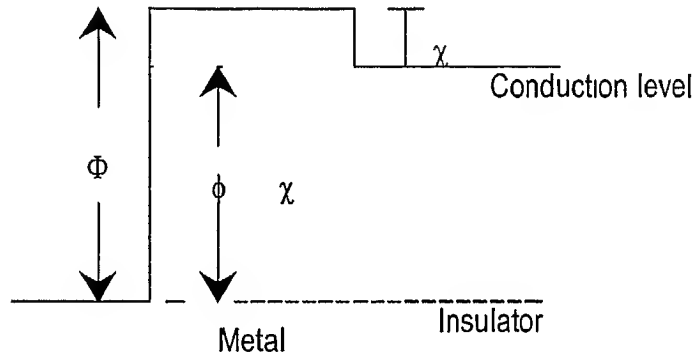
2.5 Space Charge Limited Current (SCLC)

Space charge limited currents in solids have been previously discussed in [9] and [10] for trap free and trap filled cases respectively. Simple theory predicts the space charge limited current can be passed through thin sheets of insulators. However two requirements need to be fulfilled in order to observe SCLC of significant magnitude

- (a) At least one of the contacts should be ohmic
- (b) Insulator must be free from trapping defects

Fig 2 3 Shows a metal insulator interface. An insulator can carry current if electrons are raised into a band of energy levels which are normally empty at room temperature. This does not generally happen unless $\Phi - \chi$ not too large compared to kT . Under above circumstances and when no external field is acting then a vapor of electrons will form in the insulator. This is called space charge. An equal positive charge will be formed on the surface of the metal. This will give rise to local field in the insulator. Dependence of current on voltage for smaller electrical fields for which space charge is important is given by the equation

$$J = \frac{9}{8} \mu_p \epsilon \frac{V^2}{L}$$



2 3 Energy Band Diagram of metal insulator

2 6 Space Charge Limited Current With Traps

Space charge limited current in solids has been discussed by Rose [10] for an insulator with traps. He shows that presence of traps not only reduces magnitude of space charge limited current but also is likely to distort the shape of the current voltage curve from an ideal square law to a much higher dependence on voltage. Theoretical model developed has been applied to OLED recently [6 8]. This process in OLED is called trap charge limited conduction (TCL). The trap energy level distribution is generally described by one of the following ways

- (i) Exponential distribution
- (ii) Discrete level

In modeling of OLED deviation of J-V curve from square law dependence to higher power dependence is often explained using exponential trap distribution. J-V relation in OLED with exponential trap distribution is given by [6]

$$J_{TCL} = N_{LUMO} q \mu \left(\frac{m\varepsilon}{N_t(m+1)} \right) \left(\frac{2m+1}{m+1} \right)^{+1} \frac{V^{+1}}{d^{2+1}}$$

2.7 Field Dependent mobility

One of the major differences between charge transport in crystals and in polymers is the presence of field dependent mobility [14-17] of the form

$$\mu = \mu_0 \exp\left(\sqrt{\frac{E}{E_0}}\right) \quad \text{Where } \mu_0 = \text{Zero field mobility}$$

In [16] hole mobility in a PPV material has been determined and was found that it was electric field dependent. OLED is modeled by coupling SCLC and field dependent mobility. This type of modeling has been done in [14]. Murgatroyd [12] was able to approximate the J-V relationship with field dependent mobility as

$$J = \frac{9}{8} \varepsilon \varepsilon_0 \mu_0 \frac{V^2}{L^3} \exp\left(0.89 \sqrt{\frac{E}{E_0}}\right)$$

Chapter 3

Simulation of single carrier device

3 1 Single carrier device

An understanding of the operation of OLED requires the knowledge of injection transport and recombination process involved. A single layer single carrier device provides a basis for the study of the charge injection and transport. This single carrier structure consists of an organic layer (MEH PPV) sandwiched between two contacts. Here the cathode is chosen such that it offers high Schottky barrier to electron. Anode is chosen such that it offers low barrier to hole. In this device hole dominates the current flow. The Barrier for electron is fixed at 1.4 eV. Fig –3 1 shows the energy level diagram of MEH PPV and metal contacts [18]

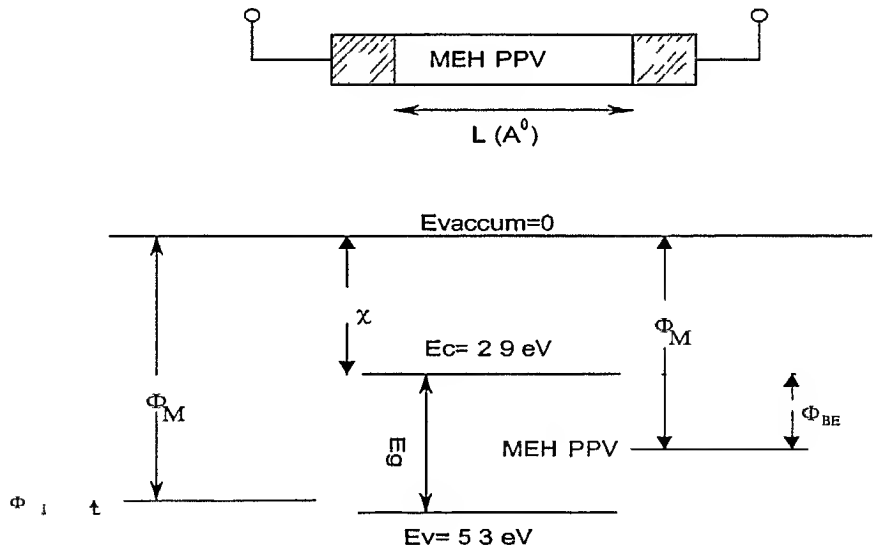


Figure 3 1 Single Carrier Structure indicating the energy levels of the organic layer and work functions of the contacts

Under forward bias the holes are injected from anode to polymer. Driven by an applied electric field these holes move through the polymer until the cathode collects them. The device operation thus involves charge injection, charge transport and collection by cathode. Schottky energy barrier for injection of holes influences current flow through the device. Hence role of the barrier in influencing the current flow needs to be investigated.

3.2 Effect of Schottky barrier on the current flow

To understand the effect of Schottky energy barrier on current flow, J-V characteristic of a 1000 Å⁰ thick device was simulated by fixing the ϕ_{BE} (barrier to electron injection) at 1.4 eV and varying the ϕ_{BH} (barrier to hole injection) from 0.05 eV to 0.35 eV in steps of 0.1 eV. The simulated J-V characteristic of the device at different values of ϕ_{BH} is shown in Fig 3.2.

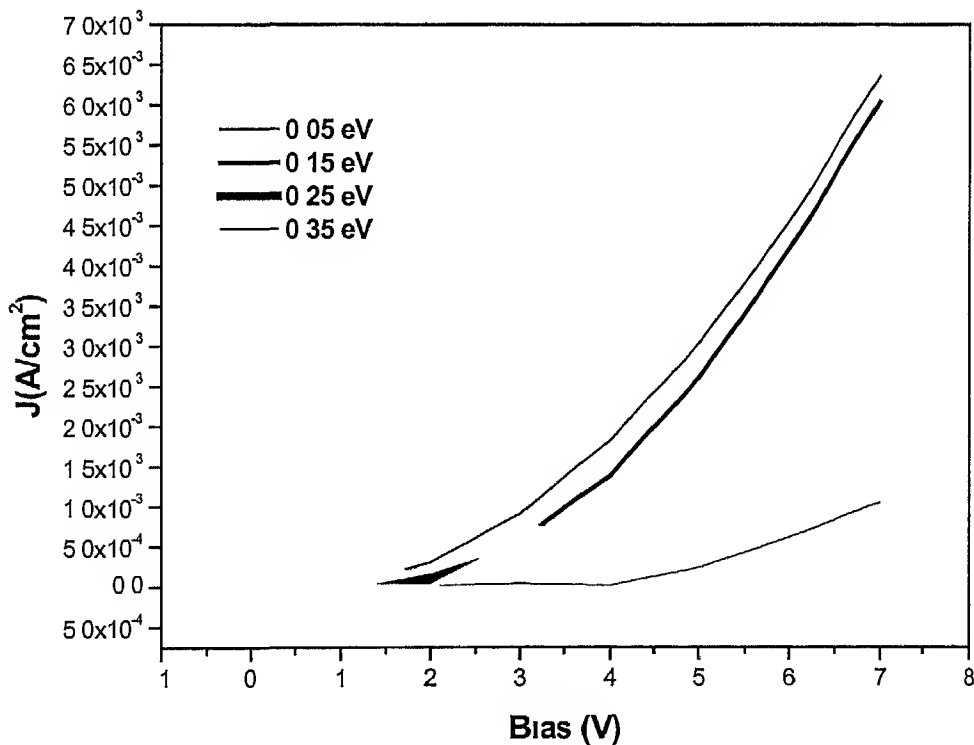


Figure 3.2 Plot of calculated current density as a function of bias voltage for a 1000 Å⁰ MEH-PPV device with 1.4 eV barrier to electron injection and 0.05, 0.15, 0.25 and 0.35 eV barrier to hole injection.

As is evident from the plot for $\phi_{BH} < 0.15$ eV curves fall almost on top of each other. However for ϕ_{BH} significantly larger than 0.15 eV the current reduces as ϕ_{BH} increases. Therefore we can conclude that for small energy barriers ($\phi_{BH} < 0.15$ eV) current flow is not limited by the contacts. But it is affected by the bulk properties of the device. Such a current flow is called bulk limited current. For energy barriers significantly larger than 0.15 eV the current flow is limited by the contact. Such a current flow is called the contact limited current or injection limited current. Hence both bulk dominated and injection dominated mechanisms influence the current-voltage behavior of polymer LEDs.

3.3 Bulk limited current-voltage characteristic

For small energy barriers ($\phi_{BH} < 0.15$ eV) current is bulk limited. J-V characteristic of the device when $\phi_{BH} = 0.1$ eV is shown in Fig 3.3. For the purpose of modeling the J-V characteristic of the device can be divided into two regions:

- (i) Low Current region ($V_{bias} < V_{bi}$)
- (ii) High current region ($V_{bias} > V_{bi}$)

Curve fitting (as shown in Fig 3.3a) in the high current region reveals that the current density J varies approximately as square of the applied bias V ($J \propto V^2$). For bias less than 1V it does not show the square dependence. This is more evident from the Log-linear plot shown in Fig 3.3b. This shows that device modeling has to be done in two separate regions.

The calculated electric field and hole density profiles are also shown in Fig 3.4 and 3.5 respectively. Hole injecting contact is to the left. Hole density in the device varies as $\frac{1}{\sqrt{x}}$. Where x is the position in the device as measured from injecting contact. Electric field in the device varies as \sqrt{x} . Since barrier for hole injection is small, holes accumulate near the injecting contact, lowering the electric field near the hole injecting contact.

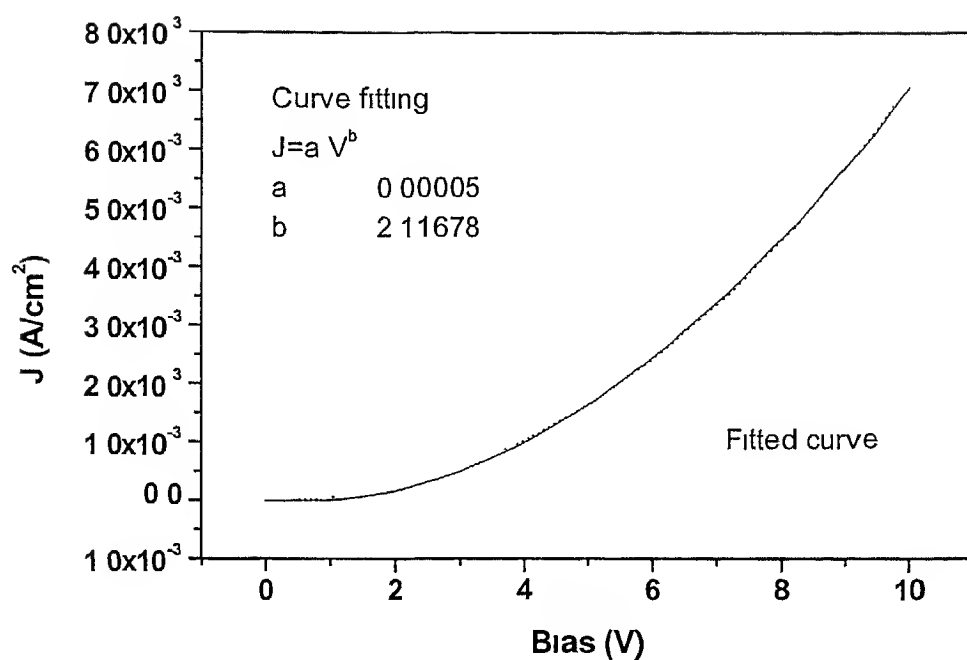


Figure 3 3a Calculated J V Characteristic of a bulk limited device

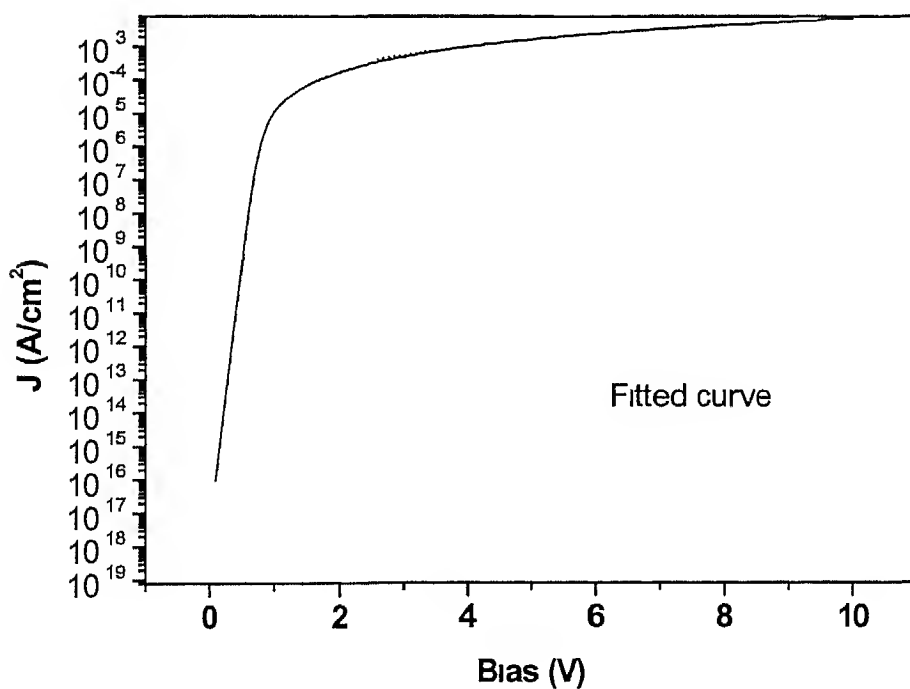


Figure 3 3b Calculated J V Characteristic of a bulk limited device (log linear scale)

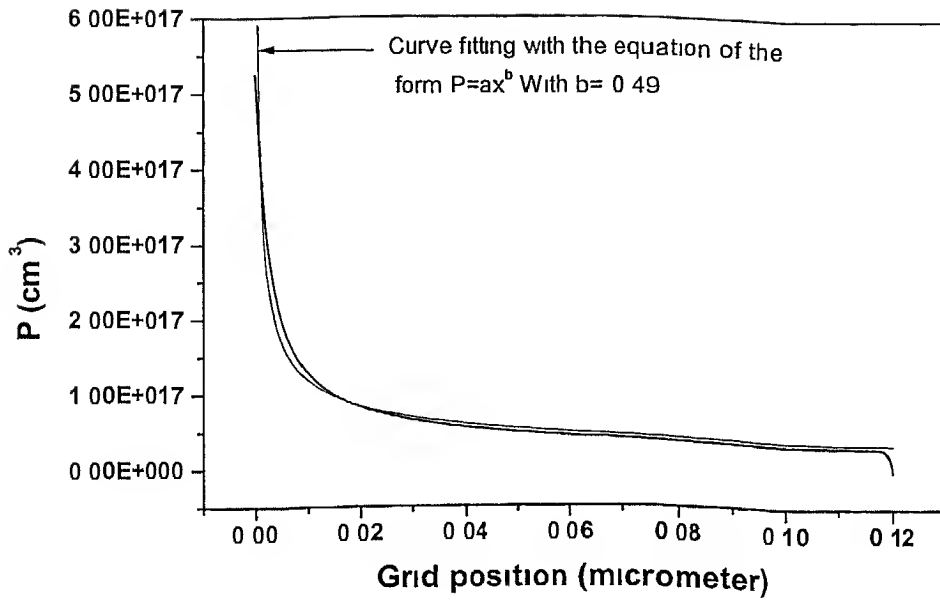


Figure 3.4 Hole density profile for a 1200 A° MEH PPV bulk limited device, at an applied bias of 4 V showing inverse of square root dependence

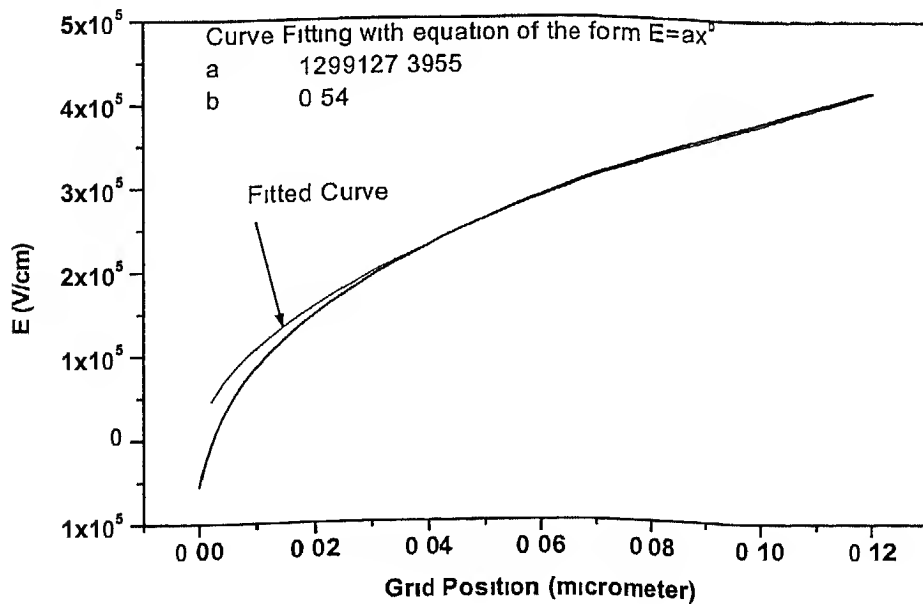


Figure 3.5 Electric Field profile for a 1200 A° MEH PPV bulk limited device, at an applied bias of 4 V , showing square root dependence of E on x

3.4 Device modeling in high current region

J-V characteristic of a bulk limited device in high current region can be modeled using theory of SCLC [9] as applied to a trap free insulator with constant mobility

$$J = J_p(x) = q\mu_p p(x)E(x) - qD_p \frac{dP}{dx} \quad 3.1$$

$$\frac{dE}{dx} = \frac{q}{\epsilon} p(x) \quad 3.2$$

Where

$$\epsilon = \epsilon_0 \epsilon_r$$

$$E = -\frac{dV}{dx} \quad 3.3$$

Substituting for p(x) from (3.2) in (3.1)

$$J = \mu_p \epsilon E \left(\frac{dE}{dx} \right) - qD_p \frac{\epsilon}{q} \frac{d^2 E}{dx^2} \quad 3.4$$

On integrating we obtain

$$J^*(x + x_0) = \mu_p \epsilon \frac{E^2}{2} - D_p \epsilon \frac{dE}{dx} \quad 3.5$$

Where x_0 is a constant of integration

Second term can be neglected if

$$D_p \epsilon \frac{dE}{dx} \ll \mu_p \epsilon \frac{E^2}{2} \quad 3.6$$

ie if applied voltage $V \gg 0.052$

$$J^*(x + x_0) = \mu_p \epsilon \frac{E^2}{2}$$

Therefore (3.5) becomes

$$E = \sqrt{\frac{2J}{\mu_p \epsilon}} (x + x_0) \quad 3.7$$

Evaluation of constant x_0

Substituting (3.7) in (3.1) and neglecting second term we get

$$J = p(x)q\mu_p \sqrt{\frac{2J(x+x_0)}{\mu_p \epsilon}} \quad 3.8$$

At $x=0$ $p(x)=P$

$$x_0 = \frac{J\epsilon}{2P_0 q^2 \mu_p} \quad 3.9$$

Evaluation of V (potential across the device)

$$E = -\frac{dV}{dx}$$

$$V_1 - V_2 = \int_0^L E dx$$

$$V = \frac{2}{3} \sqrt{\frac{2J}{\mu_p \epsilon}} [(L+x_0)^{\frac{3}{2}} - x_0^{\frac{3}{2}}] \quad 3.10$$

For small V (voltage at which space charge effect exists $V_b < 25$ V) J is small and $x_0 \ll L$

Therefore (3.9) becomes

$$J = \frac{9}{8} \mu_p \epsilon \frac{V^2}{L} \quad 3.11$$

It can be observed from the above equation that current density J varies as square of the applied voltage. Also it can be observed from equation 3.7 and 3.8 that the Electric field varies as \sqrt{x} and hole density varies as $\frac{1}{\sqrt{x}}$. These results match with the simulation results. Hence it can

be concluded that high current region can be modeled using theory of space charge limited current (SCLC)

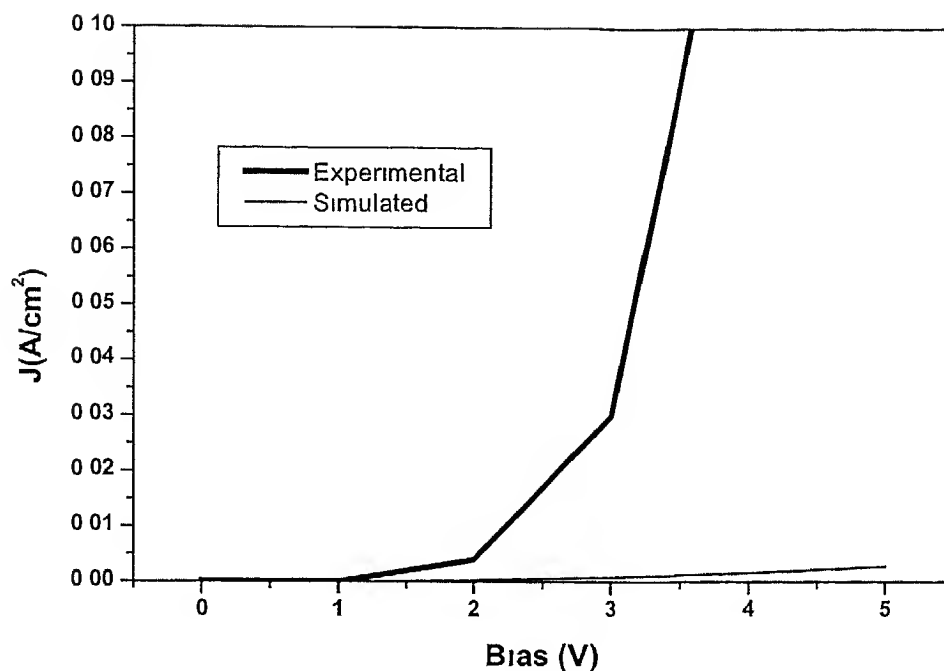


Figure 3 6a Comparison of simulated (constant mobility) and measured current density vs bias for a 1000 Å thick Pt/MEH PPV/Al device (Experimental data taken from [3])

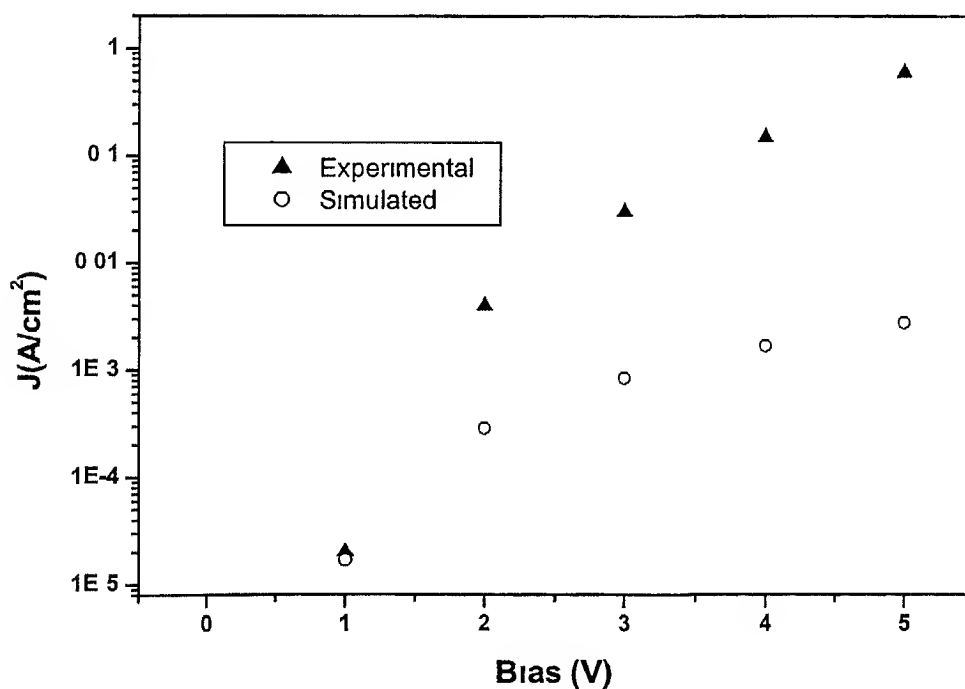


Figure 3 6b Comparison of simulated (constant mobility) and measured current density vs bias for a 1000 Å thick Pt/MEH PPV/Al device (Log Linear scale)

3 5 Experimental and simulation results

The simulated J V characteristic of a Pt/PPV/Ca device that obeys SCLC (with constant mobility) is presented in Fig 3 6a and in Fig 3 6b along with the experimental result of the same type of the device From the plots it can be observed that experimental current density is larger than that predicted by simulations This suggests that carrier mobility has increased with the electric field If the field dependent mobility of the form $\mu = \mu_0 \exp(\sqrt{\frac{E}{E_0}})$ is used in simulation then match between experimental and simulated result becomes better Fig 3 7 illustrates this point Value of the parameters used were $\mu_0=0.5 \times 10^6$ cm²/V s and $E_0=1 \times 10^5$ V/cm This result shows that hole conduction in PPV can be adequately described by combining theory of SCLC and field dependent mobility

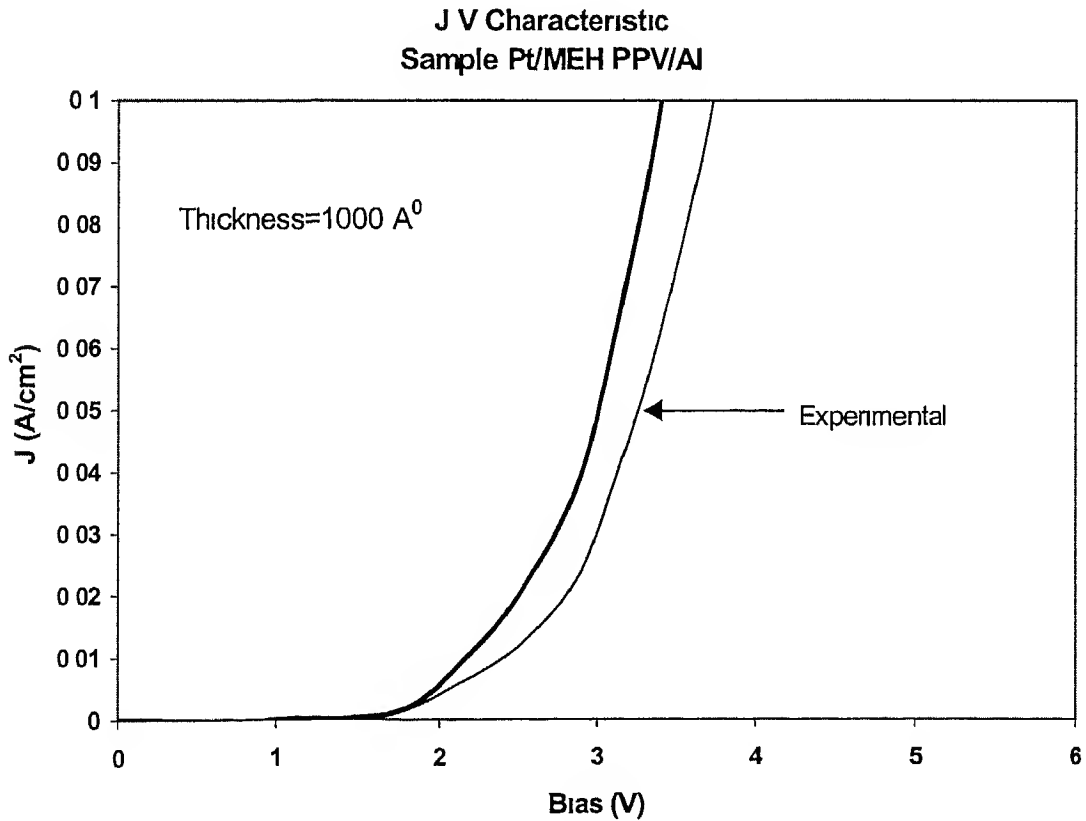


Figure 3 7 Comparison of the calculated (using theory of field dependent mobility) and measured current density vs bias for a 1000 Å thick Pt/MEH PPV/Al device (Experimental data taken from [3])

For the field dependent mobility of the form $\mu = \mu_0 e^{\sqrt{\frac{E}{E_0}}}$ there is no analytical solution for the current density Murgatroyd [12] was able to show that for field dependent mobility trap free space charge current can be well approximated by

$$J = \frac{9}{8} \varepsilon \mu_0 \frac{V^2}{L^3} e^{0.89 \sqrt{\frac{V}{LE}}} \quad \text{(Murgatroyd Model)}$$

The above expression gives only the maximum current that can be carried through the device and does not describe the higher power dependence of V on J as seen in characteristic of OLED in bulk limited regime. The development of closed form expression is facilitated by using simpler mobility model of the form $\mu = \mu_0 \left(\frac{E}{E_0} \right)^n$. The new mobility model fits reasonably well with the accurate mobility model for n=1.6. It is shown in Fig 3.8

3.6 Model for SCLC with field dependent mobility

Let us assume that mobility is field dependent of the form $\mu = \mu_0 \left(\frac{E}{E_0} \right)^n$

Using approximation of equation 3.6 in equation 3.4 as done previously for SCLC and substituting

the field dependent mobility of the form $\mu = \mu_0 \left(\frac{E}{E_0} \right)^n$

We get
$$J dx = \frac{\varepsilon \mu_0}{E_0} E^{n+1} dE \quad - \quad 3.11$$

On integrating both sides we get

$$E = \left(\frac{E_0^{n+1} (n+2)}{\varepsilon \mu_0} J (x + x_0) \right)^{\frac{1}{n+2}} \quad 3.12$$

Where x_0 is constant of integration

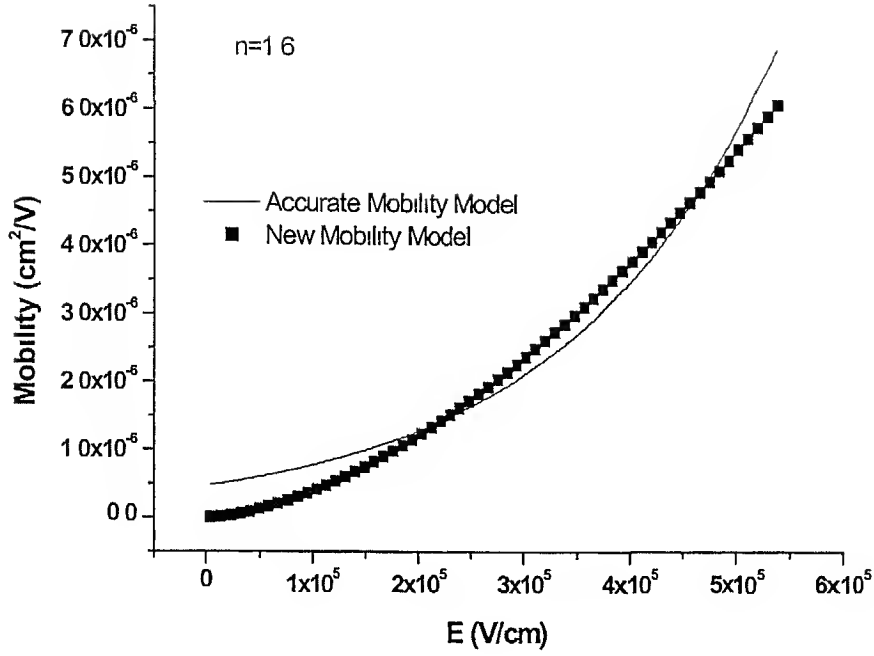


Figure 3.8 Mobility model of the form $\mu = \mu_0 \left(\frac{E}{E_0} \right)^n$ fitted to mobility model of the form

$$\mu = \mu_0 e^{\sqrt{\frac{E}{E_0}}} \quad \text{Value of } n=1.6 \text{ Evaluation of constant of integration}$$

Substituting 3.12 in 3.1 and neglecting second term of 3.1 and substituting field dependent mobility we get

$$J = \frac{P(x)q\mu_0}{E_0} \left(\frac{E_0 (n+2)}{\varepsilon\mu_0} J(x+x_0) \right)^{\frac{n+1}{n+2}} \quad 3.13$$

Applying boundary conditions

At $x=0$ $P(x)=P_0$

Equation 3.13 can be solved to get x_0

$$x_0 = \frac{\varepsilon\mu_0}{E_0 (n+2)} J^{\frac{1}{n+1}} \left(\frac{E_0^2}{P_0 q \mu_0} \right)^{\frac{n+2}{n+1}} \quad 3.14$$

Evaluation of V (Potential drop across the device)

$$E = -\frac{dV}{dx}$$

$$V_1 - V_2 = V = \int_0^L E dx$$

$$V = \int_0^L \left(\frac{E_0 (n+2)}{\epsilon_0 \mu_0} J(x+x_0) \right)^{\frac{1}{n+2}} dx$$

On Integration we get

$$V = E_0^{\frac{1}{n+2}} \left(\frac{J(n+2)}{\epsilon_0 \mu_0} \right)^{\frac{1}{n+2}} \frac{1}{\left(1 + \frac{1}{n+2}\right)} \left[(L+x_0)^{\frac{n+3}{n+2}} - x_0^{\frac{n+3}{n+2}} \right] \quad 3.15$$

For small V J is small and x_0 is small $x_0 \ll L$ equation 3.15 can be approximated

$$\text{as } V = E_0^{\frac{1}{n+2}} \left(\frac{J(n+2)}{\epsilon_0 \mu_0} \right)^{\frac{1}{n+2}} \frac{1}{\left(1 + \frac{1}{n+2}\right)} \left[(L)^{\frac{n+3}{n+2}} \right]$$

$$V^{n+2} = E_0^{\frac{n+2}{n+2}} \left(\frac{J(n+2)}{\epsilon_0 \mu_0} \right) \frac{1}{\left(1 + \frac{1}{n+2}\right)^{n+2}} (L)^{n+3} \quad 3.16$$

Equation 3.16 can be solved for J

$$J = \frac{\epsilon_0 \mu_0}{E_0 (n+2)} \left(1 + \frac{1}{n+2} \right)^{n+2} \frac{V^{n+2}}{L^{n+3}} \quad 3.17 \text{ (New Model)}$$

Equation 3.17 describes the trap free SCLC model with field dependent mobility

Comparison of J V characteristic using equation 3 17 with the experimental curve is shown in

Fig 3 9 It can be seen that analytical model predicts OLED characteristic well

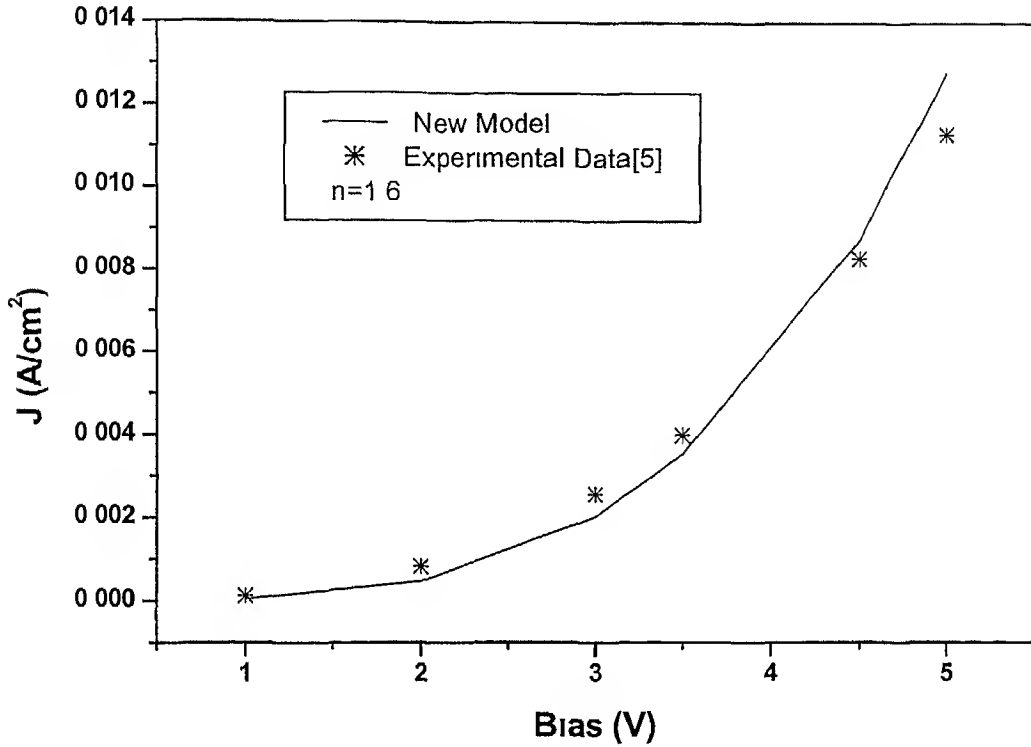


Fig 3 9 Plot showing comparison of J V characteristic obtained using the new model and experimental result

3 7 Device modeling in the low current region

Till now modeling in high current region was discussed. In low current region ($V_{bias} < V_{bi}$) dependence of current density J on applied bias V is different than that in the high current region. At low voltage region total current is sum of drift and diffusion current. In this case both drift and diffusion currents are important. **Fig 3 10** shows these two components for an applied bias of 0.2V. Direction of drift current were opposite to that of diffusion current. They are almost equal except near the cathode. As bias voltage increases drift and diffusion currents are opposite and equal to each other only in a fraction of the device. This suggests that device can be divided into two regions: Region 1 in which current components are equal and Region 2 where current components differ significantly.

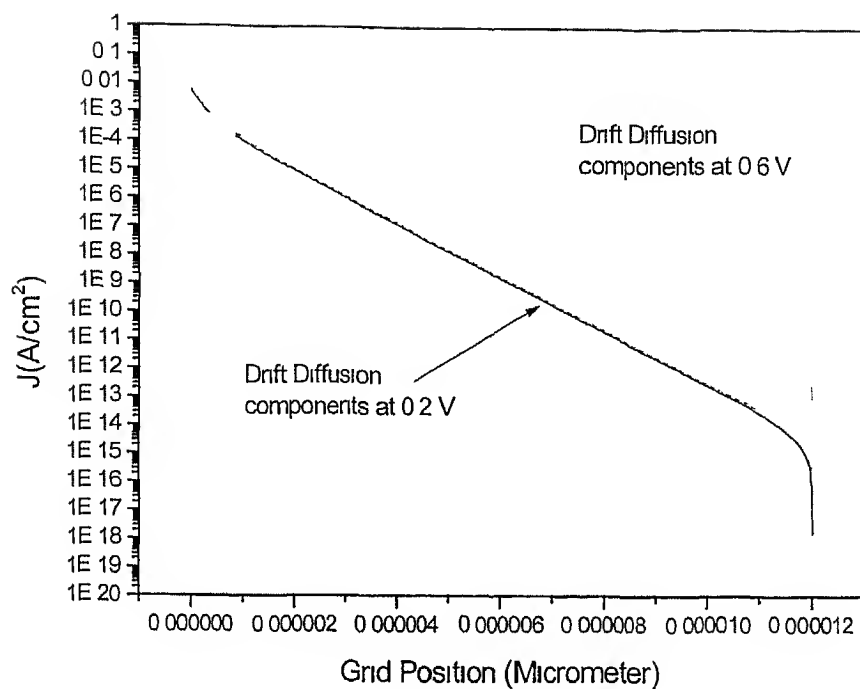


Figure 3 10 Drift and Diffusion current components at an applied bias of 0.2 V and 0.6 V

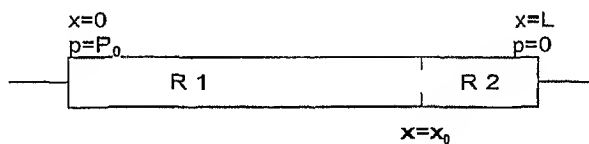


Fig 3 11 Cross section of the device

It is expected that the current flowing in the device is proportional to hole concentration at the boundary between two regions

In Region 1 drift and diffusion current components are equal

$$-q\mu_p p(x)E = q\mu_p \frac{kT}{q} \frac{dp}{dx} \quad (3.19)$$

Electric field in most of the bulk is constant because of low hole density in the bulk (Fig 3.12)
Therefore

$$E = E_0 = \frac{V - V_b}{L}$$

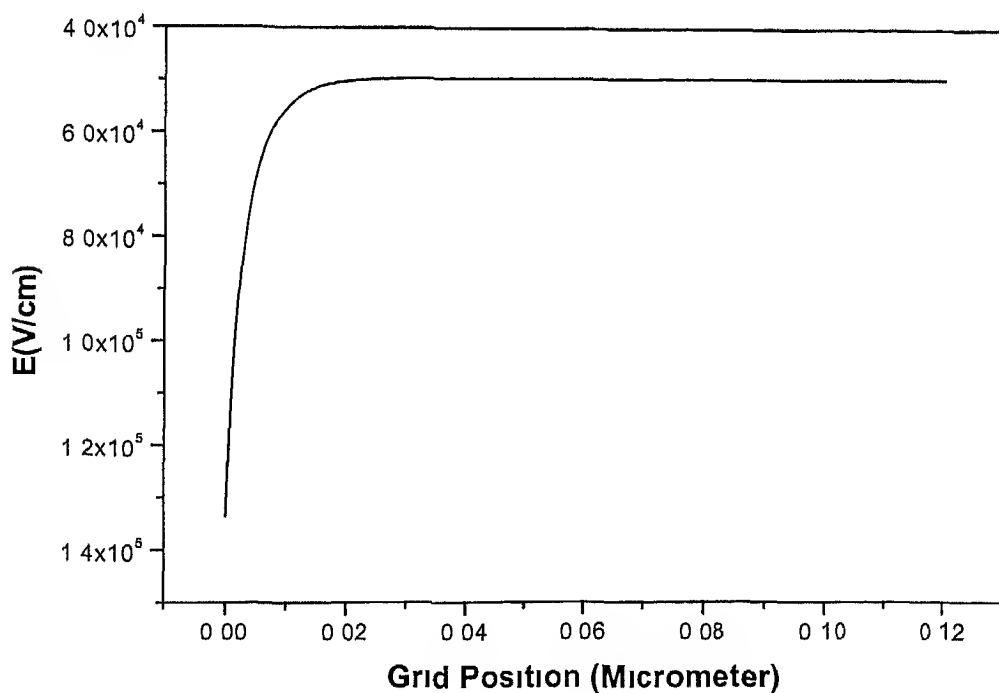


Figure 3.12 Electric Field profile of MEH PPV device at an applied bias of 0.2 V

$$\begin{aligned}
 -p(x)E_0 &= \frac{kT}{q} \frac{dP}{dx} \\
 \frac{kT}{q} \frac{dP}{dx} + p(x)E_0 &= 0
 \end{aligned}
 \tag{3 20}$$

With boundary conditions

$$\text{At } x = 0 \quad p(x) = P_0$$

Solution of which is given by

$$p(x) = P_0 \exp\left(-\frac{q}{kT} \frac{x}{L} V_0\right) \tag{3 21}$$

$$\text{Where } V_0 = |V - V_b|$$

As already stated the current in the device is expected to be proportional to $P(x_0)$

So that

$$J = -q\mu_p E_0 P_0 \exp\left(-\frac{1}{\eta V_i} V_0\right) \tag{3 22}$$

Where

$$\begin{aligned}
 \eta &= \frac{L}{x} \text{--- IdealityFactor} \\
 V_i &= 0.026V
 \end{aligned}$$

Thus from equation 3 23 it can be concluded that at low voltages dependence of current on voltage is exponential Current density J is proportional to P_0

3.8 Contact limited current flow ($\phi_{BH} > 0.15$ eV)

We have already seen that the Schottky barrier (ϕ_{BH}) at the injecting contact limits the current flow in a single carrier device when the barrier is greater than 0.15 eV. For $\phi_{BH} > 0.15$ eV, J is a function of ϕ_{BH} . With the increase of ϕ_{BH} , current density J decreases. A single layer device was considered in which the ϕ_{BH} was fixed at 0.6 eV. Schottky barrier for the electron was kept at 1.4 eV. Simulated current density using theory of field dependent mobility along with the experimental data is presented in Fig 3.13. From the plot it can be seen that measured current is greater than the current predicted by the simulation. This is because $J \propto \exp(-\frac{q\phi_b}{kT})$ and the barrier height ϕ_b is lowered by the image force effect according to

$$\phi_b = \phi_{b0} - \sqrt{\frac{qE(0)}{4\pi\epsilon}} \quad 3.24$$

ϕ_{b0} Injection Barrier at Zero Field

$E(0)$ Electric Field at the contact

Hence barrier height lowering has to be taken into effect. Taking barrier height lowering into effect, current was calculated and plotted in Fig 3.14, which is in qualitative agreement with the experimental result.

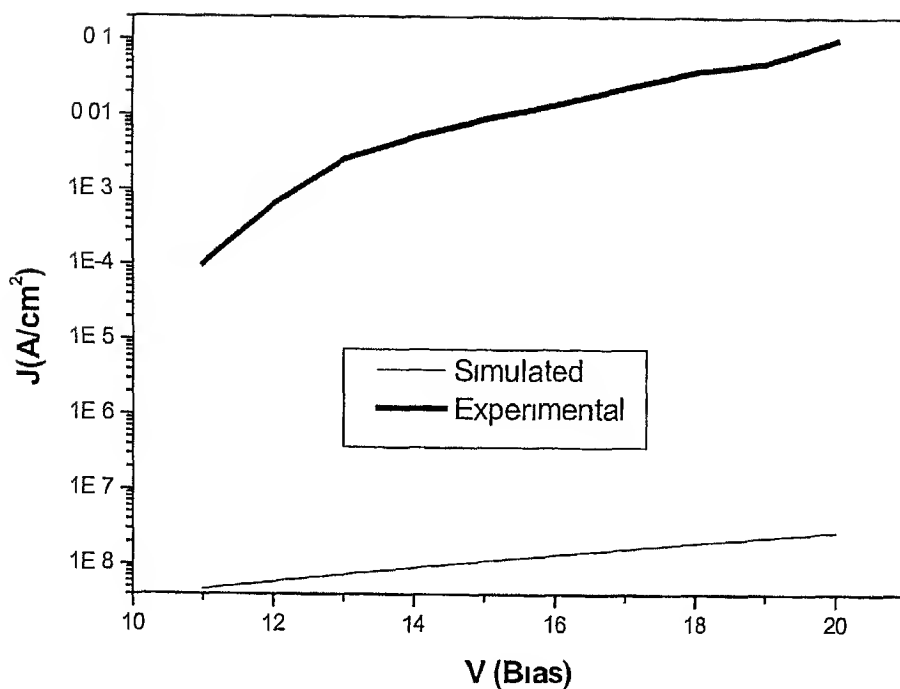


Figure 3 13 Experimental and simulated (without taking barrier height lowering into effect) J V characteristic of ITO/MEH PPV/Al device

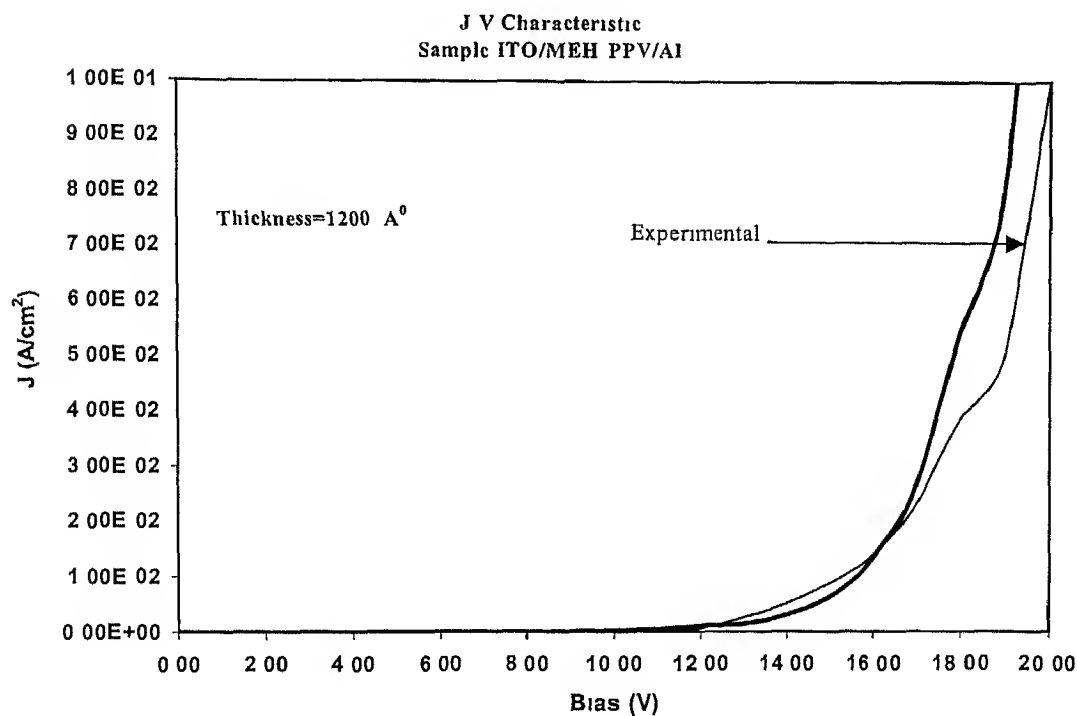


Figure 3 14 Experimental and simulated (taking barrier height lowering into effect) J V characteristic of ITO/MEH PPV/Al device

In a contact limited device hole density and electric field profile in the device are completely different from that of a bulk limited device. Calculated hole density and electric field profiles are shown in **Fig 3 15** and **Fig 3 16** respectively. When the barrier for hole injection is large, injected hole density will be very less.

$$\frac{dE}{dx} = \frac{q}{\epsilon} p(x) \cong 0$$

This infers that electric field in the device is constant. Total current through the device which is constant and is given by the expression

$$J = q\mu_p p(x)E = \text{Constant}$$

This implies hole density within the device should be constant. This argument explains the shape of the electric field and hole density profile of a contact limited device. This is also seen in simulation result shown in **Fig 3 16**.

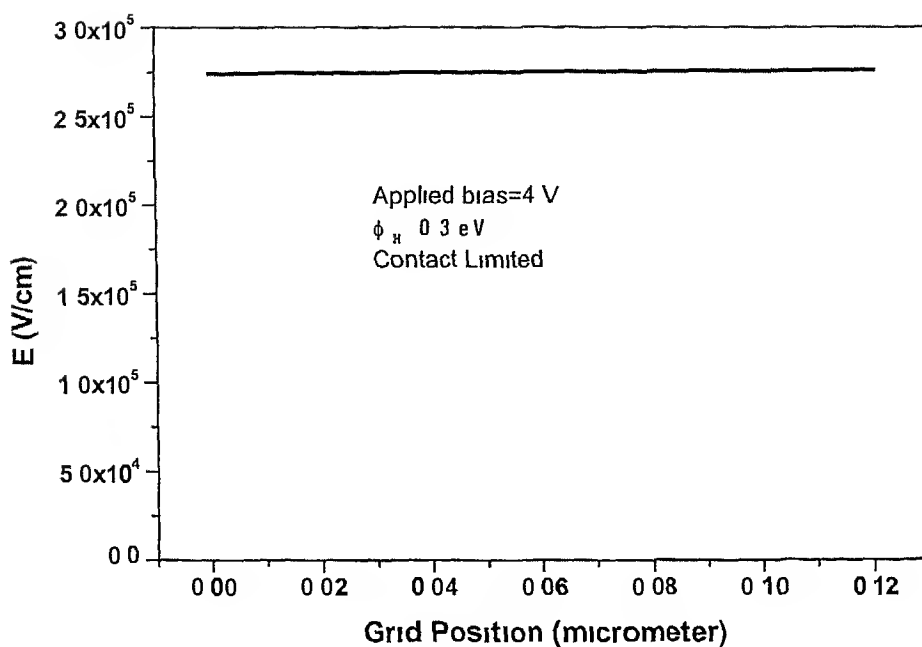


Figure 3 15 Electric Field profile for a 1200 A⁰ device in contact limited regime (with hole barrier of 0.3 eV) at an applied bias of 4 V

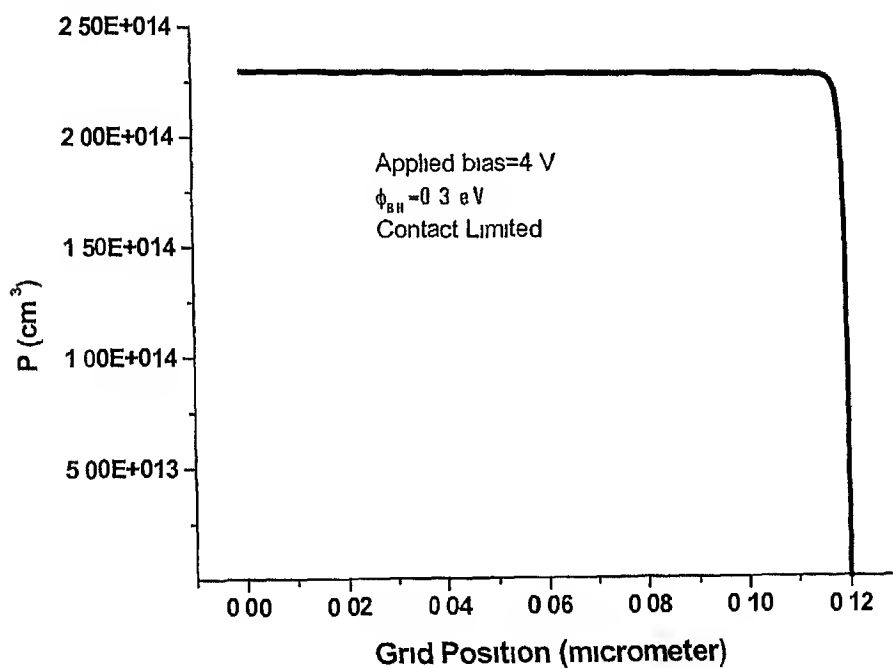


Figure 3 16 Hole density profile for a 1200 A⁰ device in contact limited regime (with hole barrier of 0.3 eV), at an applied bias of 4 V

3.9 Criteria for distinguishing bulk limited and contact limited current

This thickness dependence can be used as criteria to distinguish between contact limited and bulk limited current. In a contact limited device, dependence of current density on voltage and thickness of the device are of the same order. Fig 3.17 and Fig 3.18 shows that dependence of current density on thickness and voltage are of the same order. Whereas in a bulk limited device, dependence of current density on thickness is one order higher than the dependence on voltage.

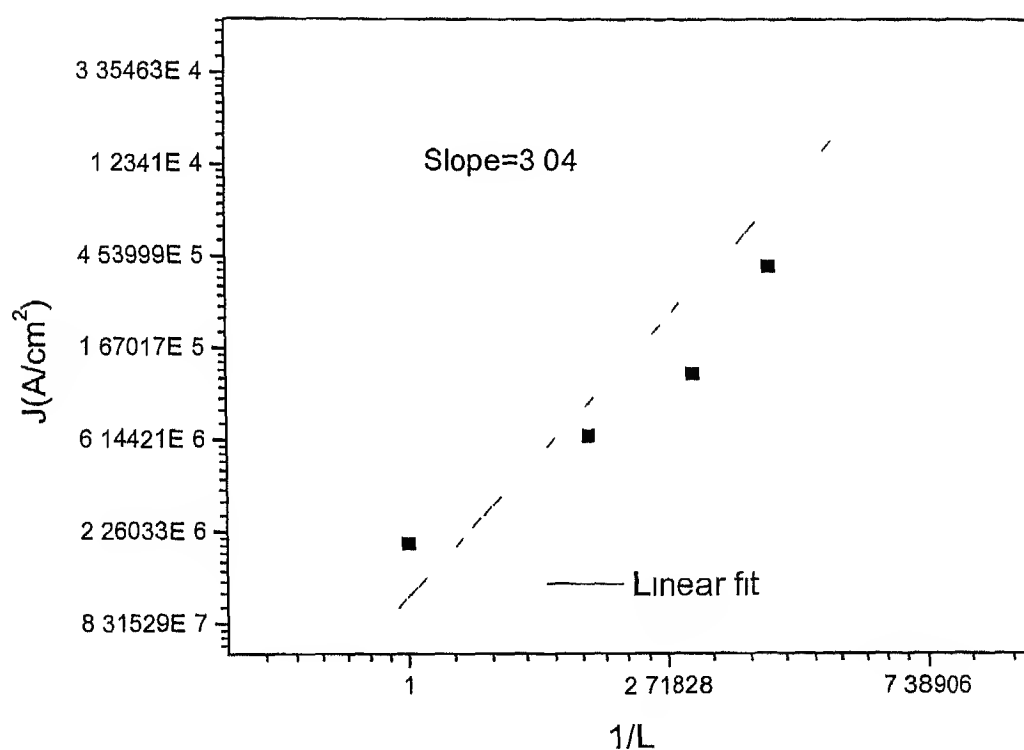


Fig 3.17 Dependence of Current on thickness of a contact limited device

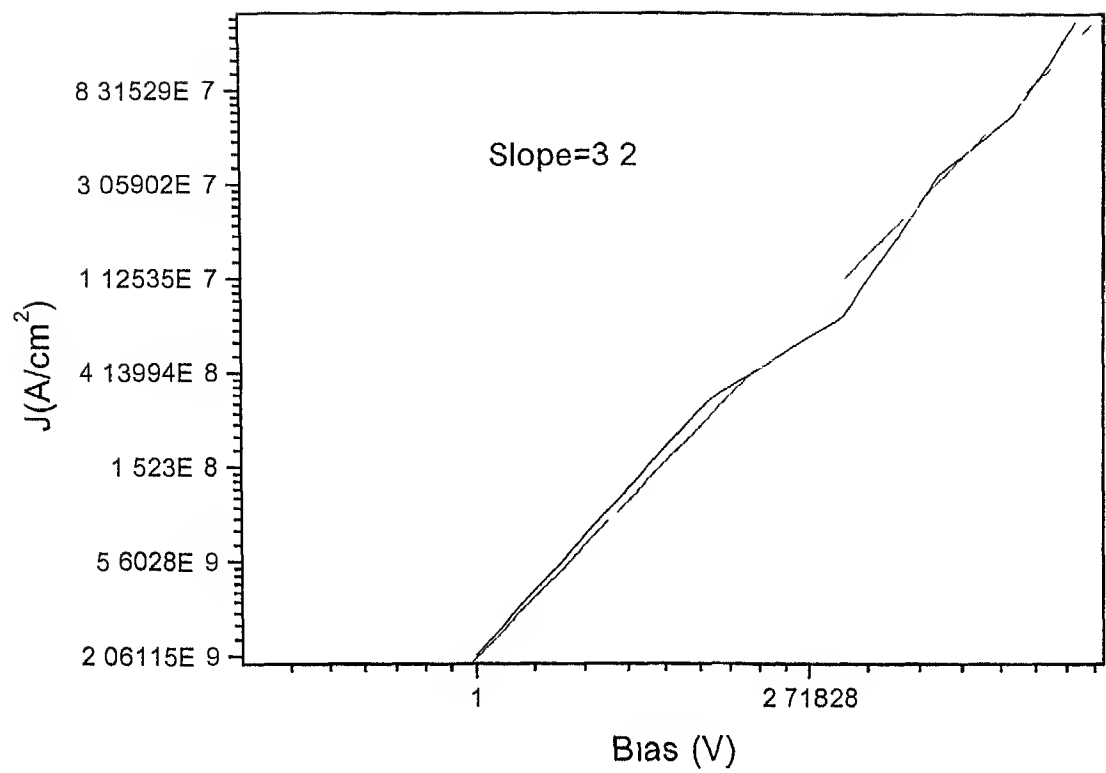


Fig 3 18 Dependence of Current on voltage of a contact limited device

3.10 Single Layer Bipolar Device

Although a mono polar device is useful for understanding the charge injection and transport mechanisms, it is the bipolar case that is of real interest because recombination and light emission takes place. In a bipolar device, holes from the anode and electrons from the cathode are injected when a voltage is applied across the device. These carriers move through the organic layer until they meet each other and recombine to form an exciton. Exciton decay may be radiative or non radiative. This process is shown in Fig – 3.19.

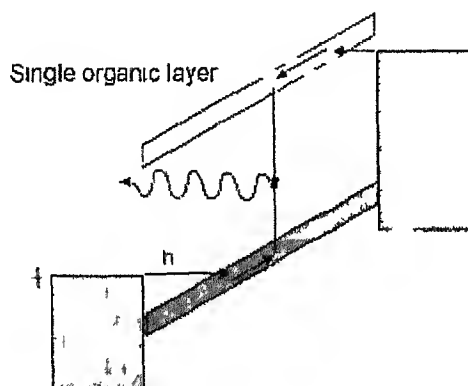


Figure 3.19 Energy Band Picture of Single Layer Bipolar Device

A bipolar device has been simulated using MEH-PPV sandwiched between Pt and Ca contacts. Pt acts as anode with the barrier of 0.1 eV for injection of holes and Ca acts as cathode with a barrier of 0.1 eV for injection of electrons. In a bipolar device, recombination has a very important role to play. Recombination affects the carrier density profile, recombination rate density profile, and luminance efficiencies.

3.11 Recombination

In bipolar device electron and hole recombine to emit light. Recombination is modeled [1] as Bimolecular of the form

$$R = np\gamma \quad (3.25)$$

Where

R Recombination rate

γ Recombination Coefficient

n, p Electron and hole density

$$\gamma = \frac{q\mu_R}{\varepsilon}$$

μ_R Effective recombination mobility which is larger of electron and hole mobility

Internal Quantum efficiency η_q of the device is given by

$$\eta_q = Q\eta$$

Where η is the recombination efficiency of the device and Q is the ratio of the radiate recombination to total recombination. Theoretical maximum value of Q is $\frac{1}{4}$. This is because of all the excitons formed $\frac{3}{4}$ are triplets and non radiative. Recombination efficiency is a measure of device efficiency. This gives the fraction of current that lead to recombination. Recombination efficiency given by

$$\eta = \frac{J_r}{J} = \frac{\text{Recombination Current}}{\text{Total Current}}$$

Recombination current is estimated from the time independent continuity equation

$$\frac{1}{q} \frac{\partial J}{\partial x} = R$$

$$\int_0^L J(x) dx = \int_0^L qR dx = J$$

Recombination current is given by

$$J_r = J_p(L) - J_p(0) = J_n(L) - J_n(0) \quad 3.26$$

Fig 3.20 shows the simulated and experimental result of a bipolar device. It is seen that simulation match well with the experimental result.

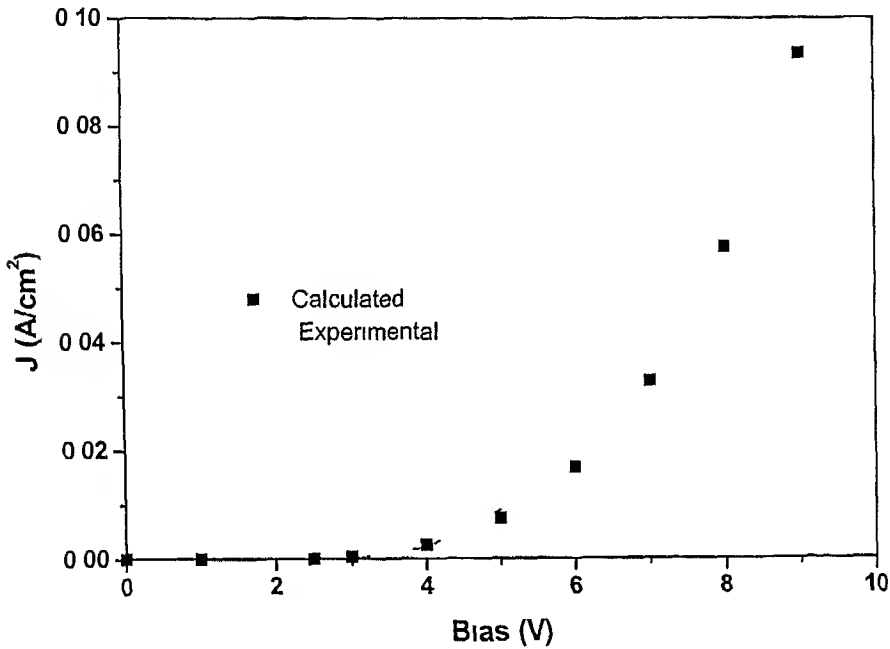


Figure 3.20 Comparison of calculated and measured current density vs bias for a 1000 Å⁰ thick Pt/MEH PPV/Ca bipolar device. Experimental data has been taken from [3]

In a bipolar device besides turn on voltage, internal quantum efficiency and device efficiency are important parameters. For the device shown in Fig 3.19, calculated internal quantum efficiency and device efficiency were 3.5% and 14% respectively. To understand the reason for such low device efficiency, recombination within the device was studied. Fig 3.21 shows that recombination is peaked near the cathode end of the device. Fig 3.22 shows the electron and hole density profile within the device. Since the electron density is significant only near the device while holes are relatively uniformly distributed, most of the recombination takes place near the cathode. Reason for this uneven distribution of the electron density is mobility ($\mu_p = 100\mu$). Fig 3.23 shows the recombination profile when $\mu_p = 10\mu$.

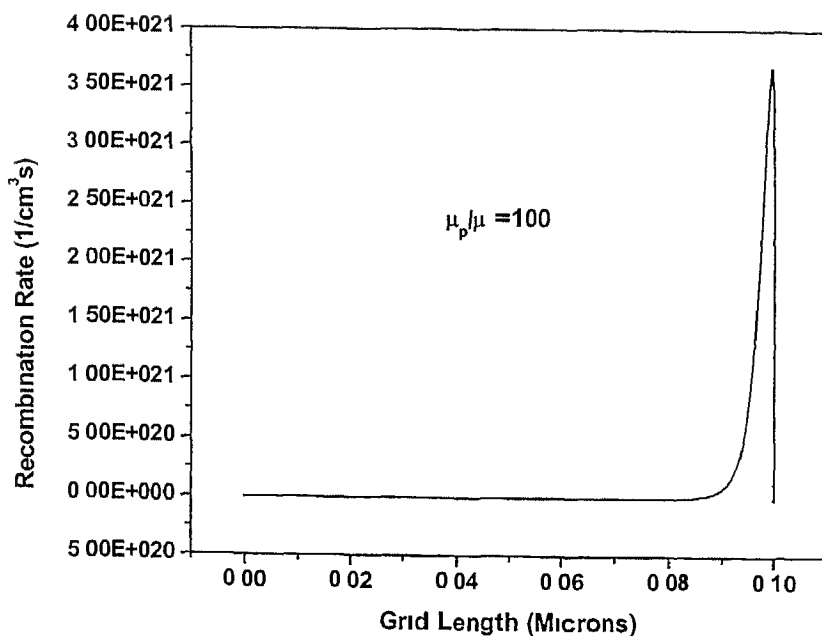


Fig 3 21 Recombination profile of Pt/MEH PPV/Ca bipolar device at an applied bias of 5 V

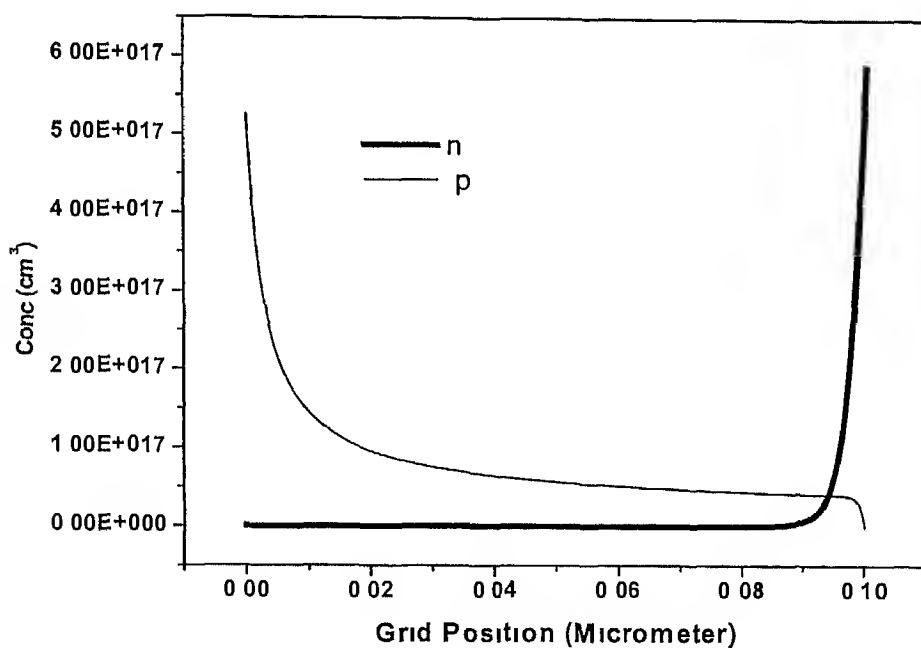


Figure 3 22 Carrier Density Profile of Pt/MEH PPV/Ca Bipolar Device at an applied bias of 5 V

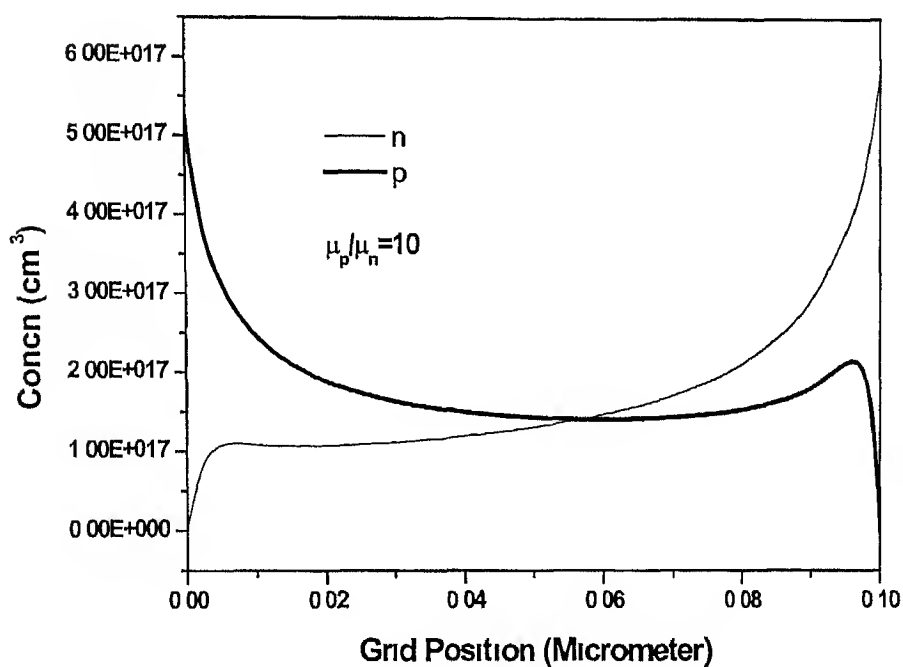
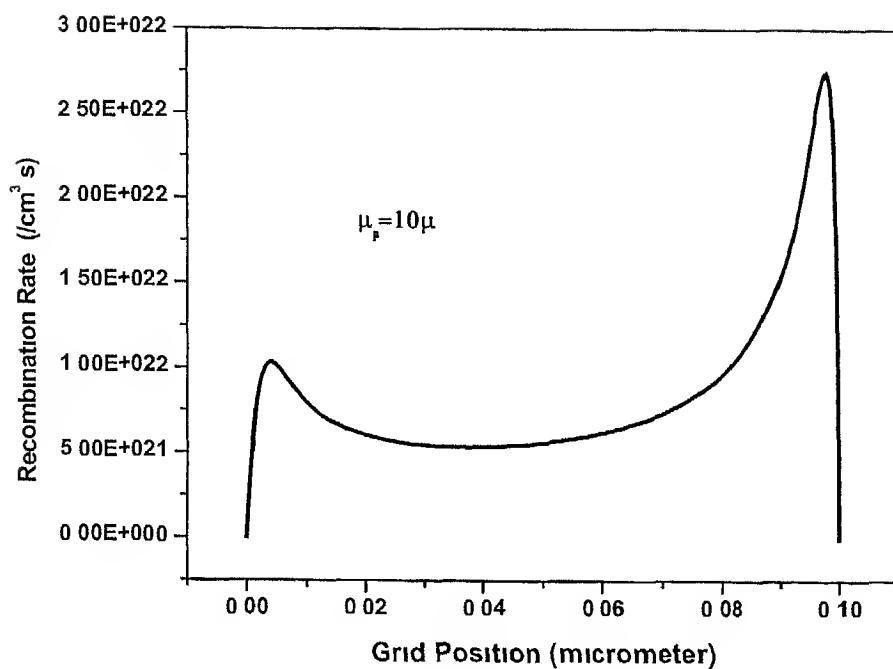


Figure 3 23 Recombination Rate and Carrier Density Profile of Pt/MEH PPV/Ca Bipolar Device at an applied bias of 5 V

3 12 Effect of Hole Injection Barrier On Recombination Rate Profile

The recombination profile within the device can be influenced not only by the mobility but also by manipulating barrier height at anode and cathode. For example Fig 3 24 shows recombination profile for varying anode barrier height. To do this recombination rate was calculated for a single layer device by varying the barrier for hole from 0 1 eV to 0 3 eV in steps of 0 1 eV. Barrier for electron at cathode was fixed at 0 1 eV. Ratio of the hole to electron mobility was maintained at 100. Applied bias was 5V. It can be seen that by increasing the barrier at anode the effect of large mobility ratio can be compensated. But this uniformity is obtained at the cost of increase in turn on voltage.

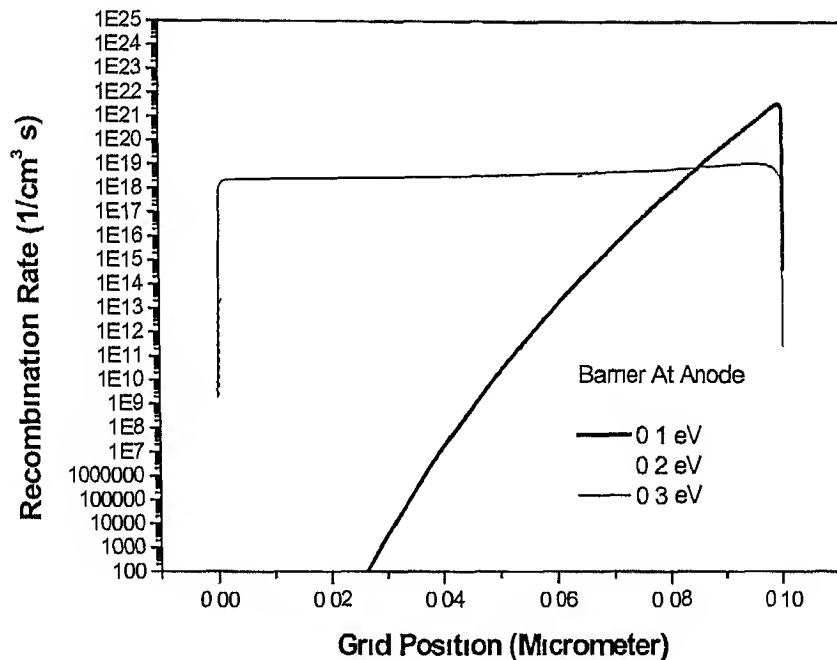


Figure 3 24 Recombination Profile of a Bipolar Device with varying hole injecting barrier. Applied bias is 5 V and ratio of mobility is 100

To conclude in a single layer device with low injecting barrier heights recombination is localized near the contact which injects low mobility carrier. This is undesirable because of quenching of the luminescence. Recombination can be moved away from the cathode using a bi layer device as discussed in next chapter.

Chapter 4

Double Layer Device

4.1 Energy Band Picture

To overcome the problems encountered in the single layer structure a double layer device is used. The structure of the device is as shown in Fig 4.1

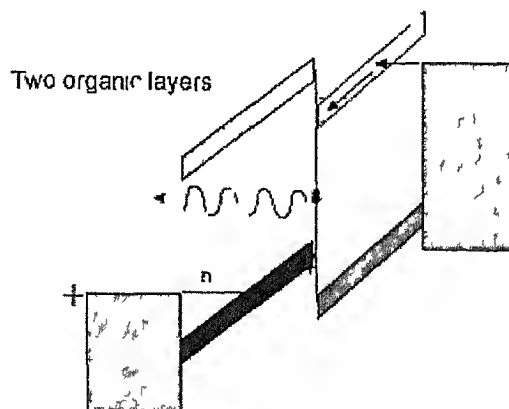


Figure 4.1 Energy Band Picture of Double Layer Structure

It consists of two organic layers. One of which is matched to the anode and transports holes with the other optimized for electron injection and transport. New layer introduced acts as a blocking and prevents high mobility holes reaching cathode. Both electrons and holes are blocked at the interface between the two layers and forced to recombine. As a result recombination occurs primarily at the interface. This is beneficial because it prevents quenching of luminescence that can occur when the recombination is near one of the electrodes.

For purpose of study a double layer device with MEH PPV/CN PPV layers was considered. MEH PPV has a band gap of 2.4 eV and CN PPV has band gap of 2.1 eV. They are used as hole and electron transport layer sandwiched between two contacts. Anode and cathode are chosen such that they offer a barrier of 0.1 eV for holes and electrons respectively. Simulated recombination profile and carrier profile is shown in Fig 4.2 and Fig 4.3 respectively. It can be seen that both hole and electron concentrations are maximum at the interface. As the rate of

recombination is proportional product of electron and hole concentrations rate of recombination is peaked at the interface Device efficiency is at it s maximum Recombination is taking place away from the injecting contact

4 2 Effect of thickness of CN_PPV layer on J-V characteristic

The variation of the potential within MEH PPV/CN PPV device when a bias of 5V is applied is shown in Fig 4 4 It can be seen that within the MEH PPV layer it varies very little compared with the variation within the CN_PPV layer This is due to difference in mobility of hole and electron It can be explained as follows We know that both electron and hole currents are drift currents

$$J_{MEH_PPV}(x) = q\mu_p p(x)E + q\mu n(x)E$$

$$J_{CN_PPV}(x) = q\mu n(x)E$$

$$(n(x) \gg p(x))$$

$$\mu_p = 100\mu$$

$$(E)_{-pp} = \frac{J_{MEH_PPV}(x)}{q100\mu (p(x) + n(x))}$$

$$\left(\frac{dv}{dx}\right)_{-pp} = \frac{J_{MEH-PPV}(x)}{q\mu n(x)}$$

The above equations shows that electric field in CN PPV is larger than MEH_PPV Therefore turn on voltage is largely determined by CN_PPV

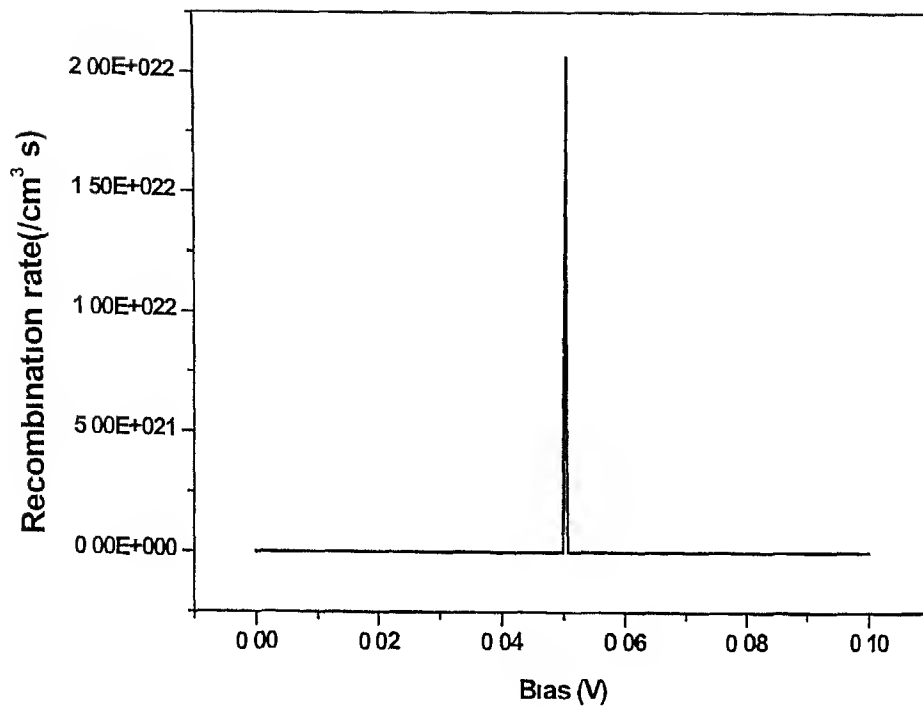


Figure 4 2 Recombination rate profile of a double layer device

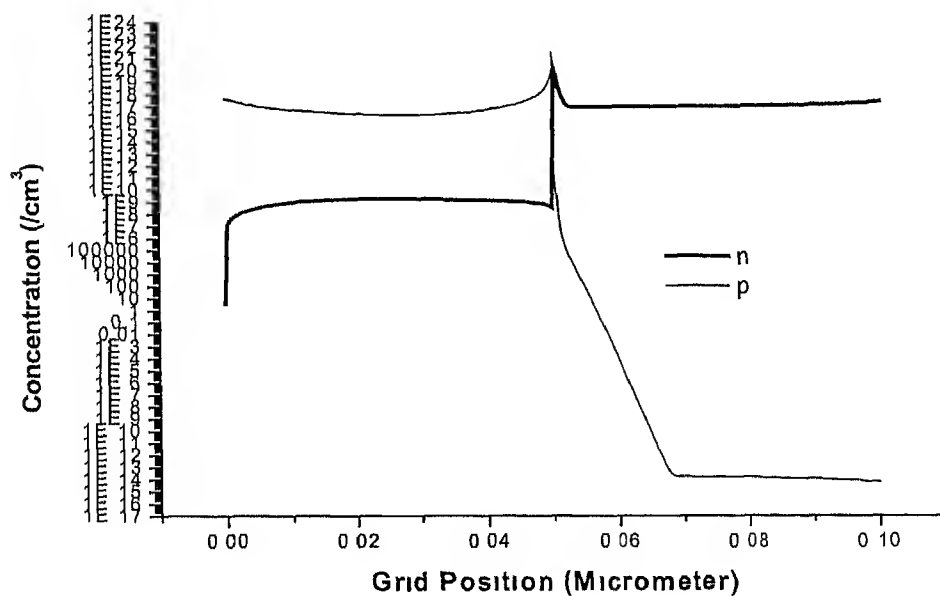


Figure 4 3 Carrier concentration profile of a double layer device

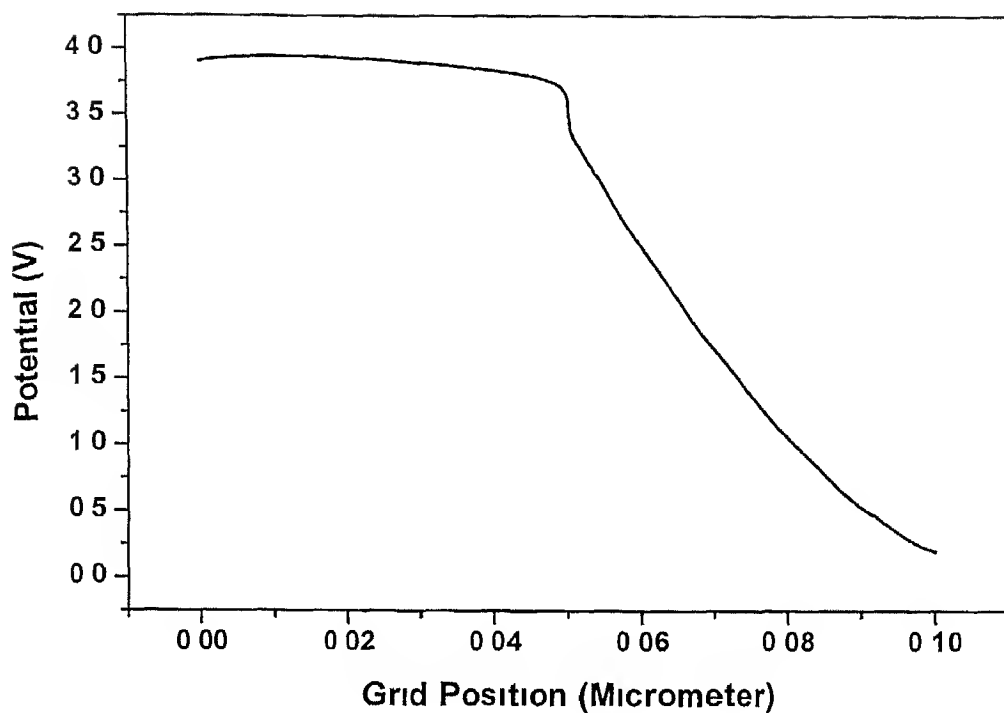


Figure 4.4 Potential Variation within MEH PPV/CN PPV Device at an Applied Bias of 5 V

DEVICE NUMBER	THICKNESS (Å)	
	MEH PPV	CN PPV
1	600	400
2	500	500
3	400	600

Table 4.1 Double layer devices of varying layer thickness

To study the influence of the CN PPV thickness three different MEH PPV/CN PPV b₁ layer devices were considered. Total thickness of all the devices was same and equal to 1000 Å but thickness of MEH PPV and CN PPV layers were different as shown in Table 4.1

The simulated J-V curve of all the three devices are shown in Fig. 4.5. From the plot, the sensitivity of the J-V characteristic to the thickness of CN-PPV layer is evident. It can be concluded that turn on voltage of the b₁ layer device is largely determined by the thickness of the electron transport layer.

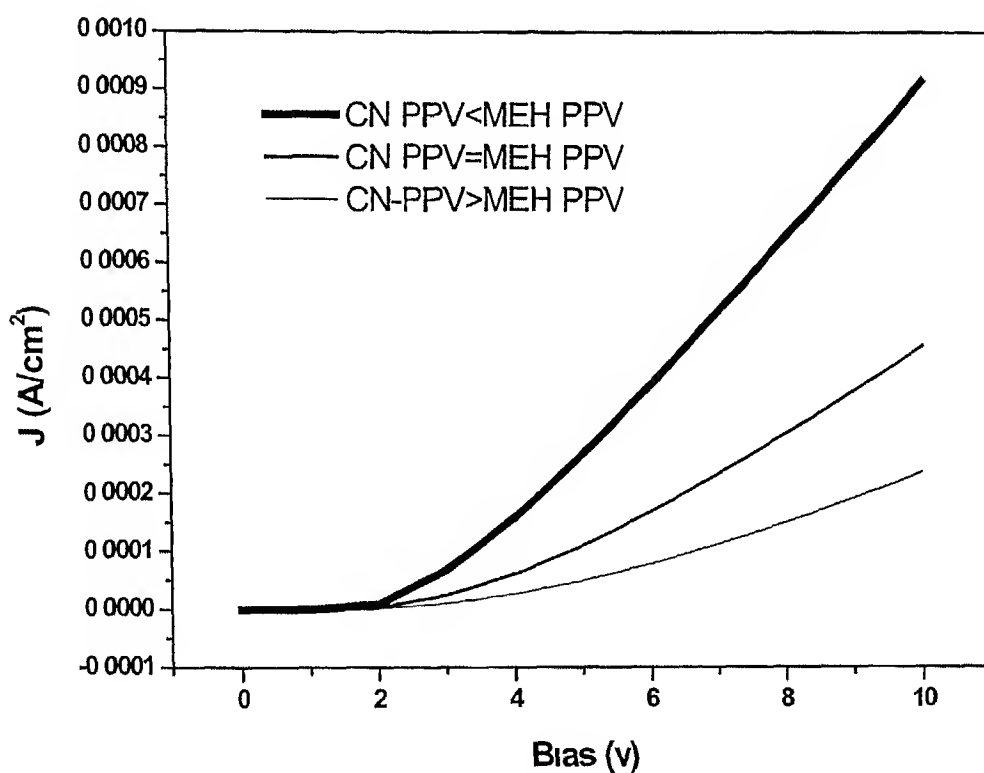


Figure 4.5 Calculated J-V Plot of the Devices 1, 2, and 3

4.3 Organic-Organic interface barrier

Band diagram of PPV and CN PPV system is shown in Fig 4.6. At the organic-organic interface, barrier to the hole injection from MEH-PPV to CN-PPV is 0.6 eV. Similarly, barrier for the electron injection from CN-PPV to MEH-PPV is 0.9 eV.

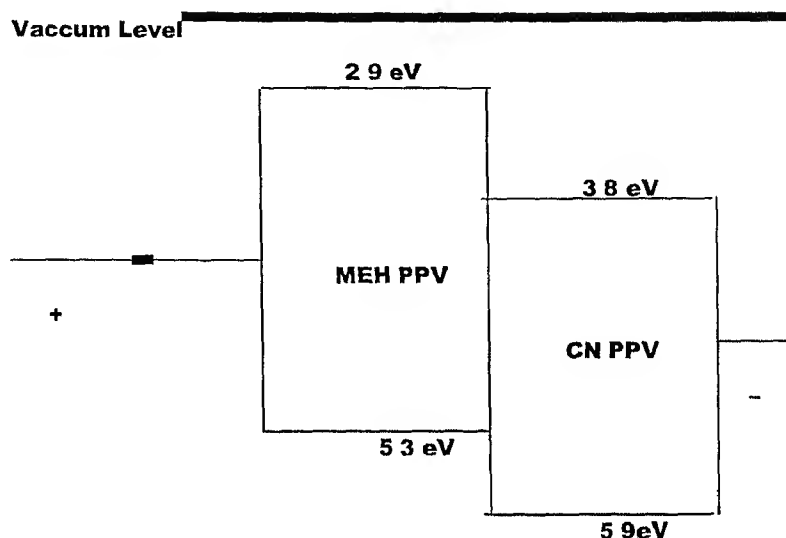


Figure 4.6 Energy band diagram of a bilayer device

To investigate the effect of hole barrier at the interface, hole barrier was reduced from 0.6 eV to 0.4 eV in steps of 0.1 eV while maintaining the hole and electron injection barriers at anode and cathode at 0.1 eV. The simulated hole density profile is shown in Fig 4.7. While on MEH-PPV side there is no variation in the hole concentration with change in interface barrier, on CN-PPV side there is an increase in hole concentration with reduction in barrier. However, this change is very small. With the reduction in hole barrier, device efficiency reduces as shown in Table-4.2. Device efficiency as a function of hole barrier is also plotted in Fig 4.8. It can be seen that to get a good device efficiency, hole barrier at the interface should be at least greater than 0.3 eV.

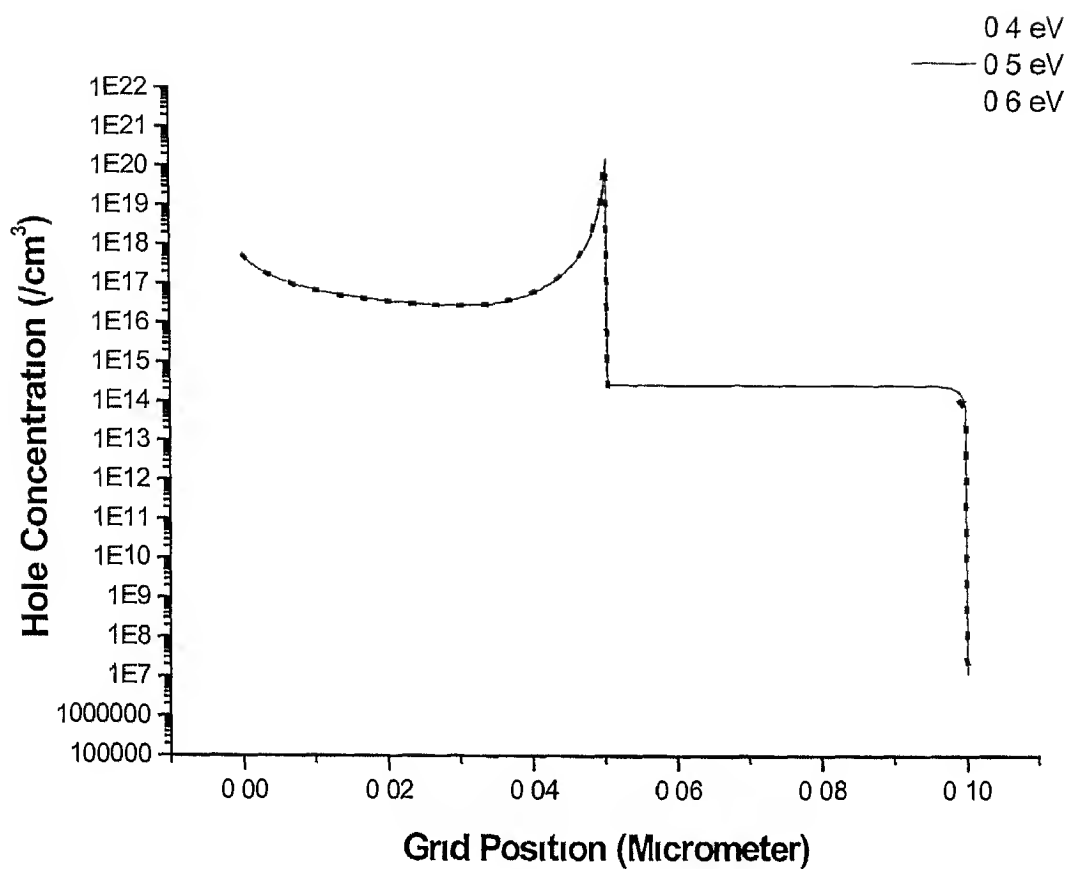


Figure 4.7 Carrier profile of a double layer at an applied bias of 5V

Organic Organic interface barrier for hole (eV)	Device Efficiency
0.6	0.98
0.5	0.95
0.4	0.91
0.2	0.45
0.1	0.15

Table 4.2 Device efficiencies at different interface hole barrier heights

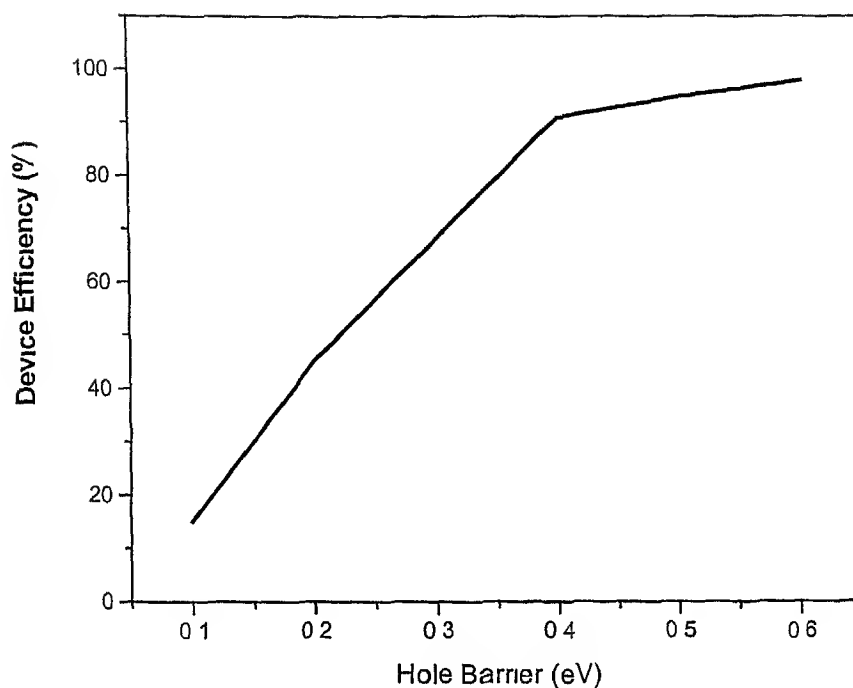


Figure 4.8 Plot of the device efficiency as a function of hole barrier at the interface

Organic Organic interface barrier for electrons (eV)	Device Efficiency
0.9	0.965
0.8	0.968
0.7	0.97
0.5	0.98
0.2	0.99

Table 4.3 Device efficiency at different interface electron barrier heights

To investigate the effect of the variation of the electron barrier at the interface, hole barrier was fixed at 0.6 eV and electron barrier was reduced from 0.9 eV to 0.2 eV in steps of 0.1 eV. The Calculated device efficiency is shown in Table 4.3. It can be concluded that electron barrier at the interface plays no significant role in influencing the device efficiency.

4.4 Comparison of Device Efficiencies of Single layer and Double Layer Devices

Efficiencies of double and single layer device were calculated at an applied bias of 5V. Thickness of all the devices was chosen to be 1000 Å.

	Anode/Barrier for hole (eV)	Organic Layer	Cathode/Barrier for electron (eV)	Device efficiency	Internal Quantum efficiency
1	ITO/0.6	MEH PPV/CN-PPV	Al/0.5	0.18	0.045
2	Pt/0.1	MEH-PPV	Ca/0.1	0.14	0.035
3	Pt/0.1	MEH PPV/CN-PPV	Al/0.5	0.009	0.0022
4	Pt/0.1	MEH PPV/CN-PPV	/0.1	1	0.25

Table 4.4 Comparison of device efficiency

Chapter 5

Conclusions

5.1 Conclusion

The J-V characteristic of OLED has been studied in detail in this work. First a single layer hole only device was studied. Using simulations the role of contact and bulk limited current mechanism was discussed. It was shown that the dependence of current on thickness could be used as a distinguishing criterion. For a bulk limited device it was shown that SCLC modified by field dependent mobility could adequately explain the experimental data. Based on simplified mobility model an analytical model for J-V characteristic was derived which agreed well with the experimental data. It was also shown that for low current region both drift and diffusion currents are important and current varies exponentially with voltage.

In a single layer device with both carrier injections recombination occurs primarily near the cathode because hole mobility is hundreds of magnitude larger than the electron mobility. The recombination profile can be spread more evenly in the bulk by reducing the mobility ratio or by reducing hole injection through increase of barrier height for hole at anode. In a two layer device both electrons and holes are prevented from reaching the opposite electrode and recombine at the interface. For high recombination efficiency the hole barrier height must be larger than 0.3 eV while electron barrier height makes no significant difference. However thickness of the electron transport layer is important in determining the OLED turn on voltage.

5.2 Application of this work

Main intention of this work was to understand device behavior using a simple 1-D device simulator. Using this work now we are in a position to predict J-V characteristic of as a function of thickness, band gap and type of the contacts. The device efficiency and quantum efficiency of the device can be predicted.

In simulations of single layer device the effect of traps on the characteristics of the device has not been examined. Modeling of the device combining theory of SCLC, field dependent mobility and trap distribution may be examined.

In simulations of single layer device the effect of traps on the characteristics of the device has not been examined. Modeling of the device combining theory of SCLC, field dependent mobility and trap distribution may be examined.

References

- 1 B K Crone P S Davis I H Campbell and D L Smith J Appl Phys **84** 833(1998)
- 2 P S Davis I H Campbell and D L Smith J Appl Phys **82** 6319(1997)
- 3 B K Crone P S Davis I H Campbell and D L Smith J Appl Phys **86** 5767(1999)
- 4 C W Tung and S A Vanslyke Appl Phys Lett **51** 913(1987)
- 5 I D Parker J Appl Phys **75** 1656(1994)
- 6 A J Campbell D D C Bradely and D G Lidzey J Appl Phys **82** 6326(1999)
- 7 B K Crone P S Davids J H Campbell and D L Smith J Appl Phys **87** 1974(2000)
- 8 P E Burows Z Shen V Bulovic D M McCarty S R Forrest J A Croin and M E Thompson J Appl Phys **79** 7991(1996)
- 9 F Mott and R W Gurney Electronic Processes in Ionic Crystals (oxford University Press New York 1940 First Edition)
- 10 Rose Phys Rev **87** 1538(1955)
- 11 Martin Pope C E Swenberg Electronic Process in organic crystals and polymers (Oxford Science Publications second edition)
- 12 P N Murgatroyd J Phys **D 3** 151(1970)
- 13 G G Malliaras and J C Scott **85** 7426(1999)
- 14 P W M Blom M J M de Jong and M G Van Munster Phy Rev **B 55** R656(1997 2)
- 15 H Meyner D Haarer H Naarman and H H Horhold Phys Rev Lett **77** 542(1996)
- 16 Jie Yang and Jun Shen J Appl Phys **85** 2699(1999)

- 17 PWM Blom M J M de Jong and J J M Vleggar Appl Phys Lett **68** 3308(1996)
- 18 I H Campbell P S Davids and D L Smith Appl Phys Lett **72** 1863(1998)
- 19 A Loannidis E Forsythe Yongi Gao M W Wu and E M Conwell
Appl Phys Lett **72** 3038(1998)
- 20 David W Winston **Simwindows** Semiconductor Device Simulator Version 1.5 1999
- 21 IBM Journal of Research and Development **45** No 1 (2001)
- 22 R H Friend R W Gymer J H Burroughs D D C Bradley Nature **397** 121(1999)

Appendix-A

Work Functions Of Contacts Used in OLED

Contact	Work Function Φ , (eV)
Ca	2.9
Al	4.3
Pt	5.2
ITO	4.8
Cu	4.6

Commonly Used Organic Materials In OLED

Organic Material	Band Gap (eV)	Electron Affinity χ (eV)
MEH PPV	2.4	2.9
CN PPV	2.1	3.8
Alq ₃	3.3	2.7
TPD	3.1	2.6

SIM WINDOWS

USER TIPS

1 Sim Windows is a 1 D device simulator originally developed for a two terminal semiconductor device. To adopt it to simulate organic two terminal devices following parameters have to be changed in material parameter file

- 1 Mobility
- 2 Band Gap
- 3 Electron Affinity
- 4 Recombination constant

Rest all parameters of the parameter file are kept at existing default values

2 In Sim Windows mobility cannot be expressed as a function of electric field. But mobility can be expressed as a function of device length. To do this at each bias voltage field is expressed as a function of x using curve fitting. Equation thus obtained is substituted in expression for mobility in the device file. This mobility in device file overrides the mobility in the material parameter file.

3 Sim windows does not incorporate barrier lowering due to image force effects. This has to be calculated externally using the electric field data. Corrected barrier height thus obtained should be used in simulation.

4 If any parameter is changed in parameter file application should be closed and restarted to make the change effective.

5 Option exists to increase the number of iterations.

A 137891

